Abdominal Radiology

Abdom Radiol (2016)
DOI: 10.1007/s00261-016-1002-6

Imaging patterns and focal lesions in fatty liver: a pictorial review

Sudhakar K. Venkatesh,[1] Tiffany Hennedige,[2] Geoffrey B. Johnson,[1] David M. Hough,[1] Joel G. Fletcher[1]

[1]Department of Radiology, Mayo Clinic, 200 First Street SW, Rochester, MN 55905, USA
[2]Department of Oncologic Imaging, National Cancer Centre, Singapore, Singapore

Abstract

Non-alcoholic fatty liver disease is the most common cause of chronic liver disease and affects nearly one-third of US population. With the increasing trend of obesity in the population, associated fatty change in the liver will be a common feature observed in imaging studies. Fatty liver causes changes in liver parenchyma appearance on imaging modalities including ultrasound, computed tomography (CT), and magnetic resonance imaging (MRI) and may affect the imaging characteristics of focal liver lesions (FLLs). The imaging characteristics of FLLs were classically described in a non-fatty liver. In addition, focal fatty change and focal fat sparing may also simulate FLLs. Knowledge of characteristic patterns of fatty change in the liver (diffuse, geographical, focal, subcapsular, and perivascular) and their impact on the detection and characterization of FLL is therefore important. In general, fatty change may improve detection of FLLs on MRI using fat suppression sequences, but may reduce sensitivity on a single-phase (portal venous) CT and conventional ultrasound. In patients with fatty liver, MRI is generally superior to ultrasound and CT for detection and characterization of FLL. In this pictorial essay, we describe the imaging patterns of fatty change in the liver and its effect on detection and characterization of FLLs on ultrasound, CT, MRI, and PET.

Key words: Fatty liver—Hepatic steatosis—Focal liver lesions—Ultrasound—CT—MRI—PET

Non-alcoholic fatty liver disease (NAFLD) is a worldwide health concern with prevalence estimates ranging from 6% to 35% and a median of 20% of adult population [1, 2] which reaches more than 90% in patients with morbid obesity and metabolic syndromes [3]. NAFLD is the most common chronic liver disease in the United States affecting about 30% of the adult population [4, 5], and the incidence of chronic liver disease due to NAFLD is increasing [6]. Moreover, metabolic syndrome is increasingly being recognized as a potential cause of NAFLD and a factor that makes regression less likely [7].

Fatty liver is also associated with a variety of metabolic disorders including alcoholism, diabetes mellitus, obesity, malnutrition, protein malabsorption, drug use, chemotherapy, hyperalimentation, cystic fibrosis, jejunoileal bypass, and inherited metabolic disorders such as acquired porphyria cutanea tarda and storage disorders such as hemochromatosis and Wilson disease [7–10].

Fatty liver is defined as the intracellular-macrovesicular accumulation of fat (triglycerides) in more than 5% of hepatocytes [11]. It is important to recognize that fatty liver is due to intracellular accumulation of fat within hepatocytes and not outside the hepatocytes like deposition and infiltrative disorders such as amyloidosis, hemosiderosis, and fibrosis. Fatty liver therefore should be ideally referred to as fatty change and not fatty infiltration. Distribution of fatty change in liver can be diffuse, focal, multifocal, perivascular, and subcapsular [8]. Diffuse fatty change in the liver is easily diagnosed on the imaging techniques—ultrasound (US), computed tomography (CT), and magnetic resonance imaging (MRI); however, atypical and focal fatty change can pose problems in distinguishing from other focal lesions of the liver.

Liver is a common site for both benign and malignant focal lesions. Focal liver lesions (FLLs) are detected by the relative differences in appearance from juxtaposed liver parenchyma and seen as different echogenicity on US, different density (attenuation) on CT, and different signal intensity on MRI. Typically, FLLs are characterized based on their appearance relative to normal or non-

Correspondence to: Sudhakar K. Venkatesh; *email:* venkatesh.sudhakar@mayo.edu

Published online: 20 December 2016

Table 1. Key points

1. Fatty change in liver is common and easily detected on ultrasound, CT, and MRI
2. Diffuse fatty change is the most common presentation but heterogeneous and variable distribution can occur
3. Focal fatty change occurs in typical locations—adjacent to ligamentum teres and periportal region
4. Nodular fatty change can mimic metastatic disease
5. Focal fat sparing is an area of liver parenchyma unaffected by fatty change in rest of liver parenchyma and occurs in typical locations—periportal and gall bladder fossa regions
6. Sonographic evaluation of focal lesions is limited in diffuse hepatic steatosis secondary to ultrasound beam attenuation
7. CT, particularly single portal venous phase has reduced sensitivity for detection of focal liver lesion (FLL) in fatty liver, especially small metastases following chemotherapy as FLLs can be similar in density to fatty liver parenchyma.
8. In patients with fatty liver, MRI is generally superior to ultrasound and CT for detection and characterization of FLL
9. Imaging appearance of FLL in fatty liver can be significantly different, and key features for characterization may not be demonstrated. For example, Presence of washout in the case of hepatocellular carcinoma and isodensity/isointensity of focal nodular hyperplasia in portal venous and delayed phases
10. Fatty livers on PET-CT show variable metabolic activity, and both focal fatty sparing (FFS) and focal fatty change (FFC) can show increased focal FDG uptake and mimic neoplastic lesions

fatty liver on both non-enhanced and post-contrast-enhanced images. The presence of fatty change alters the liver parenchyma appearance on all conventional imaging modalities and therefore, detection and characterization of FLL may pose unique challenges as current methods are optimized for the non-fatty liver. In this pictorial review, we will describe the different imaging patterns of fatty change and the effect of fatty liver on both detection and characterization of FLL on US, CT, MRI and PET. The key points of the review are summarized in Table 1.

Fatty liver: imaging appearance

The appearance of fatty liver is highly variable on US. Fatty change in the liver leads to increased parenchymal echogenicity (Fig. 1) with posterior shadowing as the fatty tissue attenuates the US beam more than normal liver. Other features include poor delineation of intrahepatic structures such as vessels and loss of definition of diaphragm [12]. However, increased echogenicity may also be seen in liver fibrosis and is difficult to differentiate from fatty change. Fatty liver is hypodense on non-enhanced CT and hypointense on opposed-phase T1-weighted MRI (Fig. 1) and on fat-suppressed MRI sequences. Uptake of gadoxetate sodium (Gd-EOB-DTPA) by hepatocytes is probably not affected by the fatty change; however, the signal intensity of the fatty liver on hepatobiliary phase fat-suppressed T1-weighted images would be significantly lower compared to that in normal non-fatty livers [13].

Quantification of fatty change

Diagnosis of fatty change with US, CT, and MRI is possible with demonstration of features described above; however, due to increasing prevalence of NAFLD, quantification of the hepatic fatty change is needed to assess the severity of fatty change, and to evaluate response to interventions to revert fatty change. Although US is a simple technique to detect fatty change, quantification on US is limited by the confounding factors of fibrosis, poor detection, and discrimination of mild fatty change and interobserver variability [14–17]. Controlled attenuation parameter (CAP) which is obtained simultaneously with stiffness measurement using transient elastography has been shown to detect mild steatosis $>10\%$ with good accuracy [18]; however, this is a relatively new technique and results from larger studies are awaited. CT can detect moderate to severe steatosis ($>33\%$ fatty change) with sensitivity of 73%–100% and specificity of 95%–100% using thresholds of <40HU attenuation of liver or a difference in attenuation between liver and spleen more than -10HU on unenhanced CT [19–22]. However, the attenuation of liver is affected by presence of other substances in the liver [22], and unfortunately there is variation in the attenuation parameter among different machines. MRI is the most accurate imaging method for quantification of fatty change. Several methods are available. Chemical shift-based In/opposed-phase imaging can be used for fat quantification [23]; however, this is limited by quantification possible only up to 50% fat signal fraction. MR spectroscopy (MRS) is considered the gold standard for fat quantification. Use of MRS needs interpretation expertise of a radiologist, and technical support of a MR physicist is required for advanced post-processing. MRS has the disadvantage of sampling error [8]. Proton density fat fraction (PDFF) estimation using chemical shift-encoded multi-echo method (IDEAL-iterative decomposition of water and fat with echo asymmetry and least squares estimation) [24] provides robust quantification of intrahepatic fat fraction. This allows for fat quantification even in the presence of moderate inhomogeneities, and quantification up to 100% is possible. Several other methods for fat quantification with MRI are described but are beyond the scope of this pictorial review, and readers are referred to detailed review articles [25–28].

Fatty change patterns

Fatty change in liver can manifest in different patterns: diffuse; geographic; focal; subcapsular; multifocal; and perivascular [8, 29, 30]. Diffuse and geographic patterns

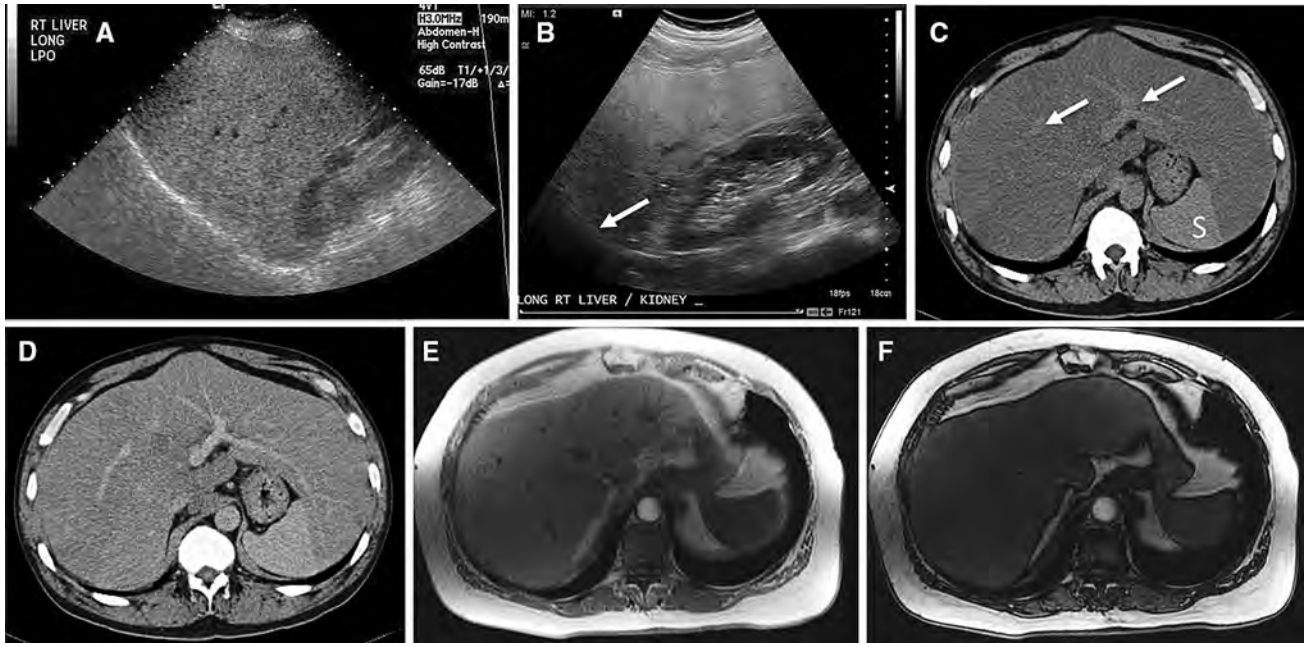

Fig. 1. Diffuse fatty change in the liver illustrated from different patients with fatty livers. Ultrasound images (**A**, **B**) of the right lobe of liver in two different subjects showing diffusely increased and coarse echogenicity of the liver parenchyma more than renal cortex and blurring of diaphragm outline (*arrow* **B**). Non-contrast-enhanced (**C**) and post-contrast CT (**D**) images showing diffusely hypodense liver due to fatty change. Note the vessels are visualized clearly on non-contrast-enhanced phase (*arrows* **C**). Liver has lower density than spleen (s). In-phase (**E**) and opposed-phase (**F**) T1-weighted gradient recalled echo MR images showing diffuse loss of signal intensity of liver parenchyma in the opposed phase consistent with diffuse fatty change.

are easy to detect; however, atypical patterns of fat deposition can pose a diagnostic challenge [29, 30]. Diffuse fatty liver results in uniform hyperechoic appearance on US and posterior shadowing if the deposition of fat is severe. On CT, diffusely fatty liver is hypodense (Figs. 1, 2) and the portal veins and hepatic veins may appear hyperdense relative to the liver parenchyma on unenhanced CT. Diffuse fatty change can be easily diagnosed on opposed-phase T1-weighted or fat-suppressed T1 and T2 sequences, which demonstrate reduced signal within the fatty liver.

Less common patterns of non-diffuse fatty change may be easily recognized once their distribution is understood. Geographic fatty change (Fig. 2) is seen as large regions of liver parenchyma with signal characteristics similar to fatty liver but being polygonal or multisegmental in distribution, or occupying more than one lobe. Geographic fatty change occurs without mass effect, possesses ill-defined borders, frequently extends to the capsule of the liver, and normal vessels course through it. Lobar and segmental fatty changes are similar to geographic fatty change but confined to lobes and segments, respectively. Subcapsular fatty change may occur in patients who receive peritoneal administration of insulin, and the clinical history of route of insulin administration should be a clue for this diagnosis [31, 32]. Perivascular fatty change is rare [30] and is due to fatty change around the portal vein and hepatic veins (or both) and demonstrates a characteristic tram-track like or tubular configuration about the vessels. MRI demonstration of fat in a perivascular location without mass effect is suggestive of this unusual pattern of fat deposition. Patterns of fat deposition that can cause diagnostic dilemmas include focal fatty change, focal fatty sparing, and multifocal nodular fatty change which are explained further below.

Focal fatty change (FFC)

Well-defined focal fatty change (FFC) can be recognized based on the typical location within the liver. FFCs are usually adjacent to falciform ligament or periportal location (Fig. 3) and are related to venous supply or venous anomalies in these regions. The abnormal accumulation of fat may be caused by relative ischemia due to decreased portal venous blood flow or decreased delivery of unknown substances from the gastrointestinal tract via the portal vein [33]. FFCs typically appear to enhance lesser than the surrounding normal liver parenchyma in hepatobiliary phase due to their fat content (Fig. 3). When FFC has nodular configuration, it may be difficult to differentiate it from a FLL (Fig. 4). This form of FFC can be challenging to differentiate from other focal lesions even with hepatocyte-specific contrast agents [34].

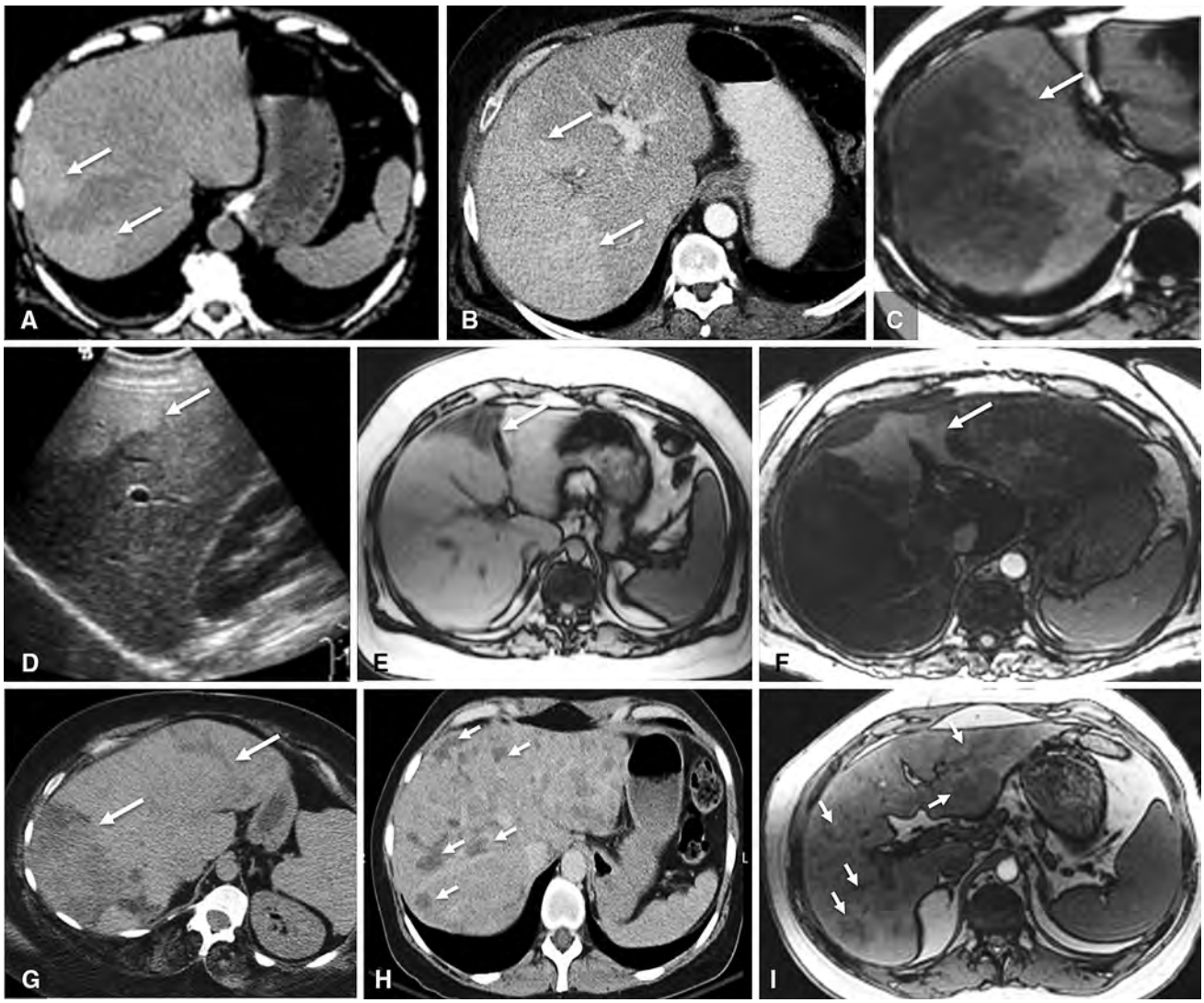

Fig. 2. Patterns of fatty change in the liver illustrated from different patients with fatty livers. Non-contrast enhanced (**A**) and portal venous phase (**B**) CT images showing geographic fatty change with sparing in peripheral right lobe (*arrows*). Opposed phase T1-weighted MR image (**C**) and ultrasound image (**D**) showing geographic fatty change (*arrows*) affecting several segments of liver. Opposed phase T1 images (**E**, **F**) showing sub segmental fatty change affecting segment IV (**E**, *arrow*) and diffuse fatty change in liver with focal fat sparing around falciform ligament (**F**, *arrow*) . Non contrast enhanced CT (**G**) showing irregular regions of fatty change in several segments (*arrows*). Contrast enhanced CT (**H**) showing multiple nodular regions fatty change (*arrowheads*). Opposed phase T1-weighted image (**I**) showing fatty change in perivascular region (*arrowheads*) and diffuse mild fatty change.

Focal fatty change can occur as a ring of steatosis surrounding liver metastases from insulinoma (Fig. 5). This is attributed to insulin secreted by the insulinoma metastasis and resulting in high concentration of local insulin and affecting the surrounding hepatocytes [31]. Patchy and segmental deposition of fat may also be seen in islet cell transplantation mirroring the distribution of harvested islet cells following injection into the portal vein.

FFCs are often termed as pseudolesions and should be differentiated from true FLLs (Fig. 6). Characteristic location, wedge or pyramidal shape, and lack of mass effect are useful features to distinguish them. FFCs tend to show variable enhancement during dynamic phase and may appear as well-defined or ill-defined hypointense lesions on hepatobiliary phase MRI with hepatocyte-specific contrast agents such as gadobenate dimeglumine (Gd-BOPTA) and gadoxetic acid (Gd-EOB-DTPA) (Fig. 3) [35].

Focal fatty sparing (FFS)

Focal fatty sparing (FFS) are regions of liver that do not show fatty change, whereas rest of the liver parenchyma

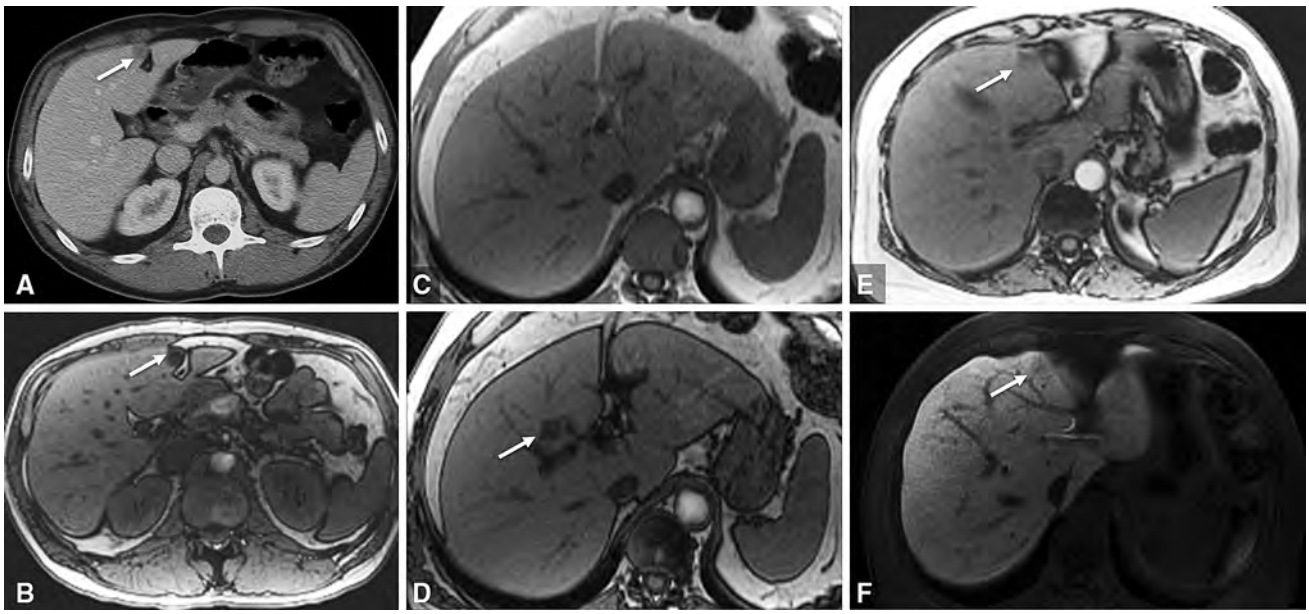

Fig. 3. Focal fatty change in the liver in different patients. Contrast-enhanced CT (**A**) and opposed-phase T1-MRI image (**B**) in a 39-year-old man showing focal fatty change adjacent to ligamentum teres (*arrows*). In-phase (**C**) and opposed-phase (**D**) MRI images in a 48-year-old woman demonstrating focal fatty change in periportal region (*arrow* **D**). Opposed-phase T1 image (**E**) and Gd-EOB-DTPA-enhanced hepatobiliary phase T1-image (**F**) in a 62-year-old woman showing focal fatty change (*arrows*). Note mild hypointensity of the focal fatty change in hepatobiliary phase.

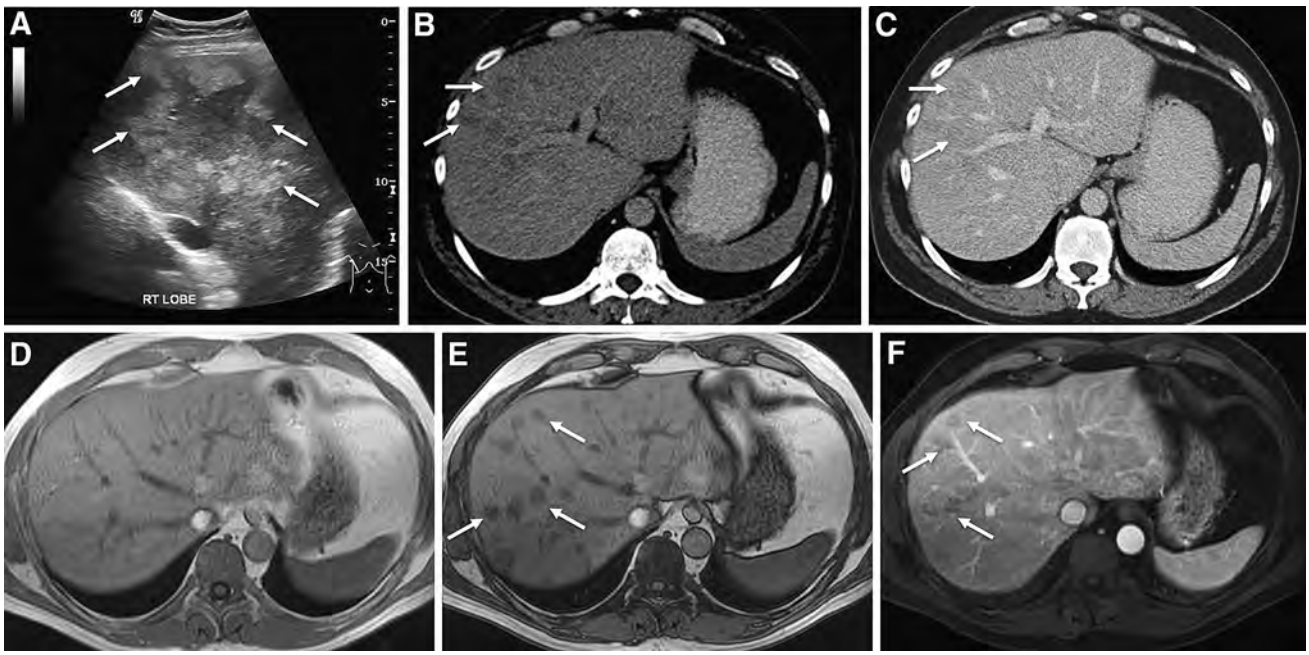

Fig. 4. Nodular focal fatty change. *Top row* **A** A 49-year-old diabetic male with incidentally detected focal hyperechoic lesions (*arrows*) in the liver on ultrasound (**A**). Note mild diffuse increase in echogenicity of liver parenchyma with nodular hyperechoic regions. Non-contrast-enhanced (**B**) and enhanced CT (**C**) showing subtle hypodensities (*arrows*) corresponding to the nodules seen on ultrasound. Histology confirmed fatty liver parenchyma from core biopsy of two of these nodules. *Bottom row* A 50-year-old male with nodular fatty change: In-phase (**D**), opposed-phase (**E**), and contrast-enhanced (**F**) MRI images showing multiple nodules of focal fatty change (*arrows*).

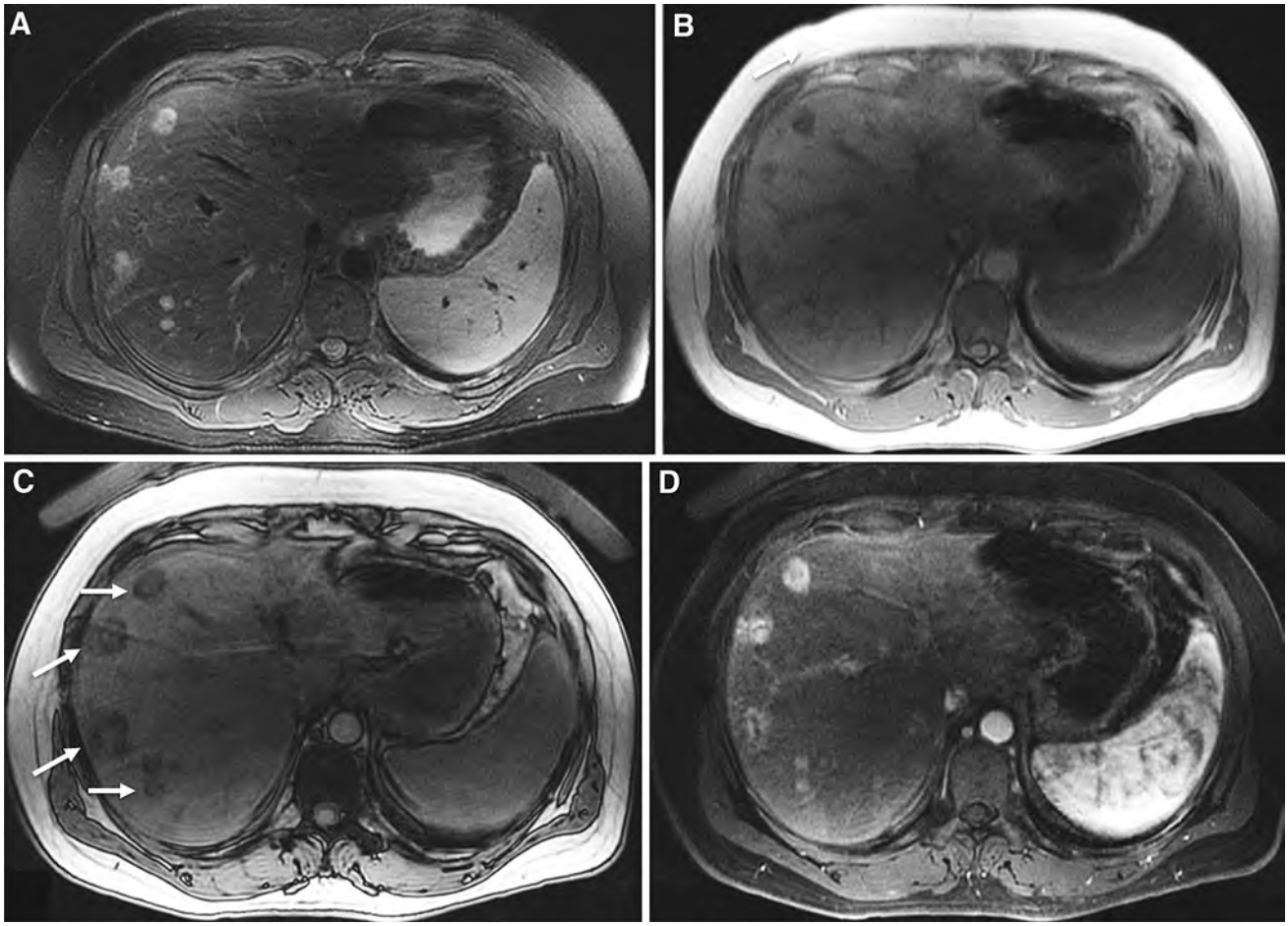

Fig. 5. Focal fatty change around lesions. A 31-year-old male with pancreatic tail insulinoma and biopsy-proven liver metastases. T2-w (**A**), in-phase (**B**), opposed-phase (**C**), and post-gadolinium-enhanced arterial phase (**D**) sequences showing multiple T2 hyperintense (**A**) lesions in the right lobe that are irregular in outline, T1 hypointense with a variable thin rim of fatty change seen as signal loss in the opposed-phase images (*arrows* **C**) and intense arterial phase hyperenhancement characteristic of these metastases. Primary tumor is not shown.

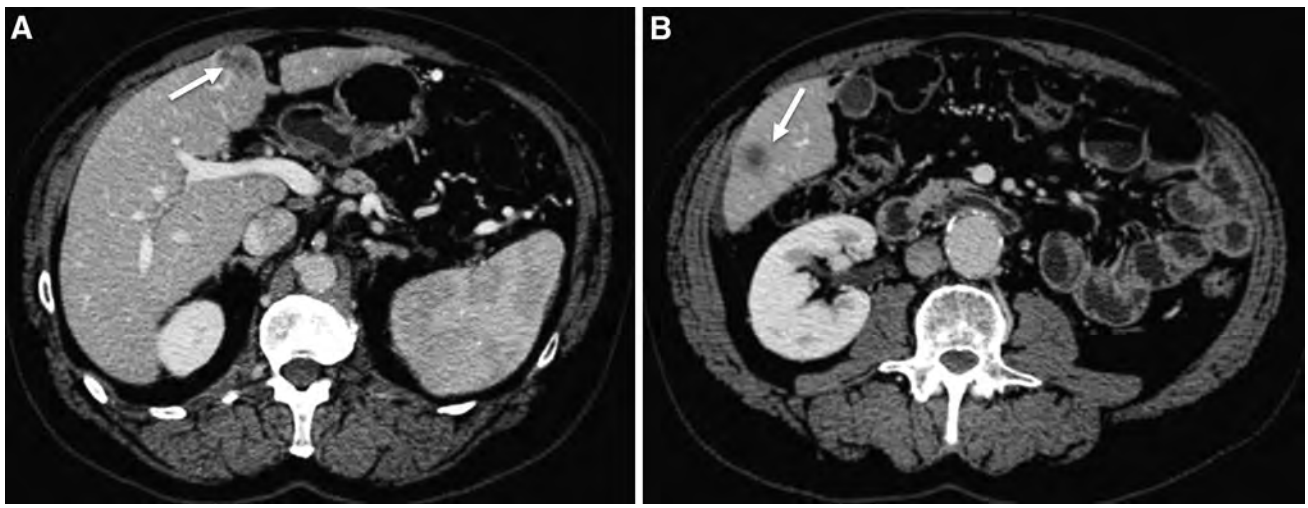

Fig. 6. Metastases occurring at typical location of focal fatty change. Patient with pancreatic carcinoma with multiple liver metastases (*arrows*). Heterogeneously enhancing and nodular lesion adjacent to ligamentum teres (*arrow* **A**) in similar location as focal fatty change (see Fig. 3). Another metastases (*arrow* **B**) in the inferior right lobe.

shows fatty change. Common locations of FFS are subcapsular location in segment IV and V, adjacent to the left portal vein or falciform ligament, near gall bladder fossa and around porta hepatis. FFS in these locations are thought to be due to decreased blood flow from main portal vein and/or associated anomalous venous drainage resulting in decreased uptake of triglycerides [36].

FFS appear hypoechoic on US, hyperdense on CT, and hyperintense on fat-suppressed MRI sequences (Fig. 7). Nodular focal sparing can mimic lesions such as adenoma or focal nodular hyperplasia [37]. FFS can also be found around or distal to a tumor (Fig. 8), potentially due to decreased portal flow, arterioportal shunting, compression of hepatic venules surrounding the tumor, and/or direct drainage of arterial blood from the tumor into the adjacent parenchyma [38, 39]. FFS occurring with liver lesions can be peripheral or distal to the lesion, segmental or lobar depending on the relationship between the focal lesion and major portal vessels [39]. Ring-shaped FFS can be seen around hemangiomas and malignant lesions such as hepatocellular carcinoma and metastases (Fig. 8) [38, 40–42]. The occurence of FFS around lesions is more frequently seen in metastases than in primary FLLs [42]. When a wedge-shaped FFS is found, a lesion at the apex of the segment and/or near the hilum should be ruled out [38].

Detection of FLLs in fatty liver

The incidence of FLLs in fatty liver is probably similar to normal liver; however, there are emerging reports and evidence suggesting increased incidence of HCC in NAFLD patients and particularly in those with steatohepatitis and occur independent of cirrhosis [43–45]. FLLs have variable appearance on US and can appear hypoechoic, isoechoic, or hyperechoic to normal liver parenchyma. The increased echogenicity of fatty liver on US often accentuates the echogenic differences with hypoechoic and isoechoic FLLs and may thereby improve the sensitivity of detection of FLLs. However, severe fatty change attenuates the US beam (Fig. 9) and smaller posterior lesions may not be detectable especially if located deep in the fatty liver. Some FLLs like hemangiomas are typically echogenic and may miss detection in a fatty liver when they are of similar

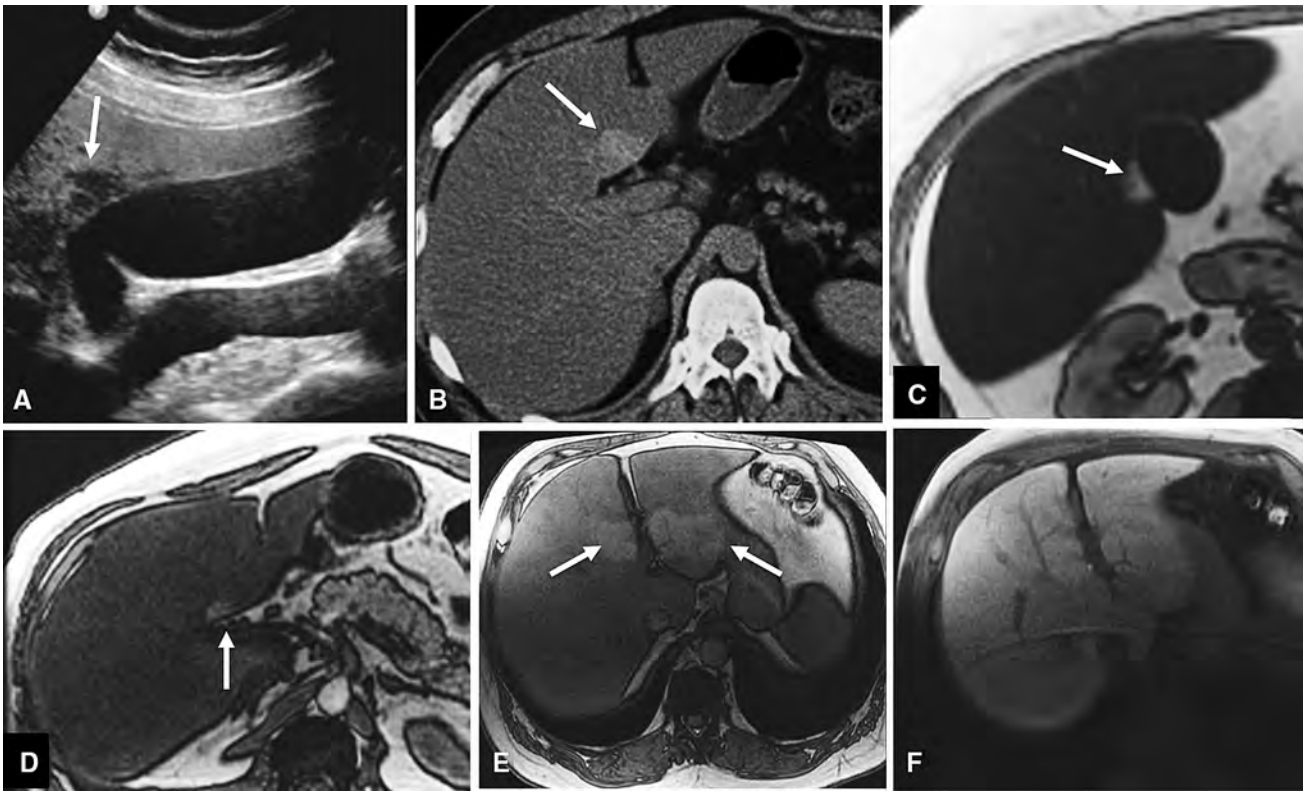

Fig. 7. Focal sparing in fatty liver demonstrated in different subjects: Focal fat sparing is seen as a hypoechoic region adjacent to the gall bladder fossa (*arrow* **A**) on ultrasound, hyperdense region in the periportal location (*arrow* **B**) on non-contrast-enhanced CT, and as a hyperintense region in the gall bladder fossa (*arrow* **C**) and periportal region (*arrow* **D**) on opposed-phase MRI images. Opposed-phase T1 image (**E**) and hepatobiliary phase image (**F**) in a 57-year-old male showing diffuse fatty change in the liver with nodular regions of fat sparing in the left lobe (*arrows*). Note the uptake of Gadoxetate like normal liver. The focal fatty sparing was stable on follow-up imaging.

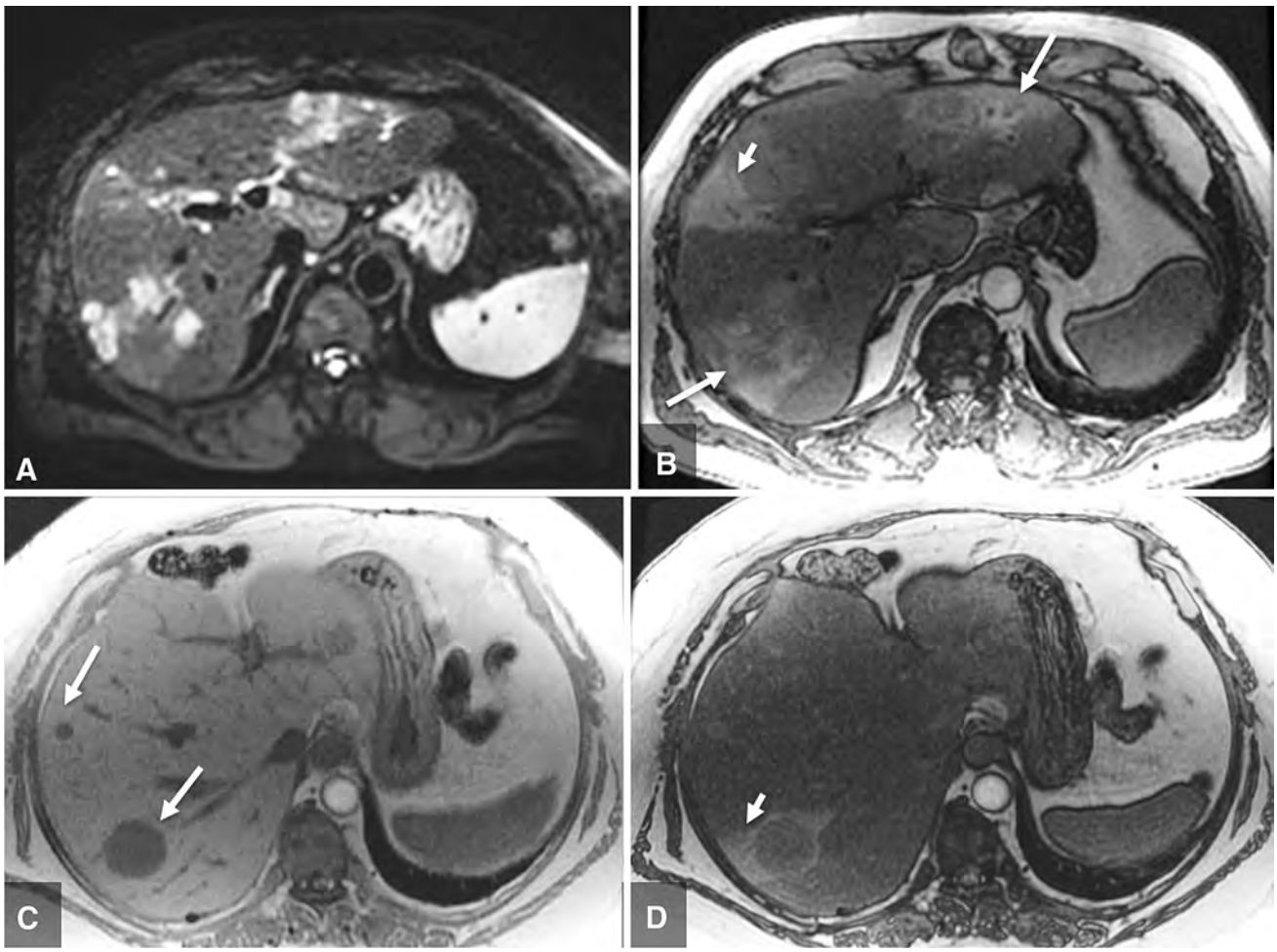

Fig. 8. Focal sparing of fatty change around and in segments peripheral to metastases. *Top row* A 55-year-old male with colon carcinoma metastases in liver. DWI image (**A**) and opposed-phase image (**B**) showing multiple lesions with diffuse fatty change and sparing around the metastases (*arrows*) and segmental regions distal to the metastases (*arrowhead*). *Bottom row* A 62-year-old male with neuroendocrine carcinoma metastases to the liver. In-phase (**C**) and opposed-phase (**D**) images showing two lesions (*arrows*) with a rim of fat sparing (*arrow head*) and peripheral liver.

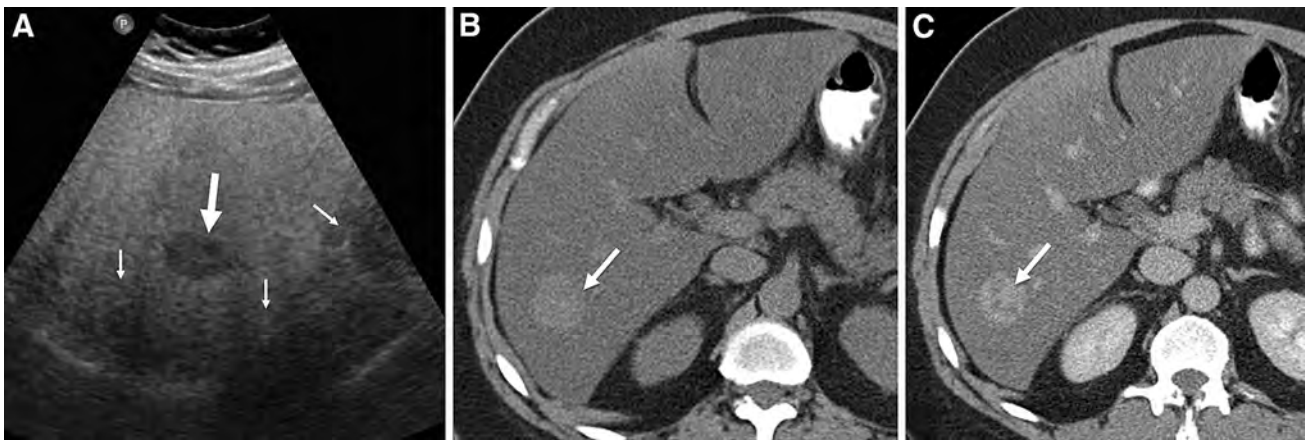

Fig. 9. Detection of focal lesion in fatty liver. Ultrasound (**A**) of a fatty liver in a 55-year-old woman with hemangioma (*arrow*) seen as a hypoechoic lesion. Note the shadowing in the posterior aspect of the liver (*small arrows*) which may obscure small hypoechoic lesions. Non-contrast-enhanced CT (**B**) showing the hemangioma (*arrow*) in the right lobe of liver and the characteristic filling in the post-contrast-enhanced delayed CT (**C**). The lesion was stable on follow-up for 2 years.

Fig. 10. Detection of focal lesion in fatty liver on CT. Baseline contrast-enhanced CT (**A**) and 18 months post-treatment (**B**) in a 52-year-old man with Hodgkin's lymphoma with liver involvement. A hypodense lesion (*arrow*) representing liver deposit was clearly demonstrable in the initial CT but diffuse fatty change in the follow-up scan makes it difficult to detect and assess the response of the lesion after treatment.

echogenicity to the surrounding fatty liver. Macroscopic fat-containing FLLs like angiomyolipoma and lipoma may be difficult to detect in a fatty liver with US for similar reasons. On CT, detection of hypodense lesions such as metastases in a fatty liver can be difficult on a single-phase contrast-enhanced CT [46–48] (Fig. 10). Often in patients with metastatic disease, livers undergo fatty change secondary to chemotherapy. Hypodense metastatic lesions when of similar density as surrounding fatty change can be potentially missed, particularly when small [46, 49]. In this setting, inclusion of unenhanced imaging, multiplanar reconstructions, or multiphasic imaging after intravenous contrast may be useful for improving lesion conspicuity and detection. MRI may provide superior sensitivity compared to CT and US as sequences with and without fat suppression can be performed that may help to detect the lesions (Fig. 11). FDG-PET may also be useful in these situations as FDG-avid lesions can be easily detected with PET-CT (Fig. 11). In patients with fatty liver, MRI is generally superior to US and CT for the detection and characterization of FLL particularly for the assessment of metastases (Fig. 12). Kulemann et al. showed that MRI is superior to CT for the detection of colorectal liver metastases after neoadjuvant chemotherapy and consecutive diffuse fatty change particularly for small lesions <1 cm [48].

Characterization of FLLs in fatty liver

The characteristic imaging features of different FLLs are described in relation to the non-fatty liver. Fatty change in the liver results in changes in echogenicity, attenuation, signal intensity, enhancement of the liver parenchyma, and thereby results in different appearances of FLLs from that classically described. Most common FLLs occuring in fatty liver are described in the following sections.

Hemangioma

Classically, hemangiomas are described as hyperechoic to isoechoic to the normal liver on US. When fatty change is mild to moderate and echogenicity similar to the hemangiomas, it may be difficult to detect them on ultrasound. A severely fatty liver with increased echogenicity, however, may provide better contrast for the detection of relatively hypoechoic hemangiomas. On CT, fatty change may improve conspicuity of hemangiomas by increasing the attenuation differences and in post-contrast scans, the peripheral nodular enhancement or delayed fill-in compared to the adjacent hypoattenuating liver parenchyma (Fig. 13). Similarly on MRI, hemangiomas may be rendered conspicuous with fat-suppressed sequences, and differences from surrounding liver may be enhanced for non-contrast-enhanced and post-contrast-enhanced sequences. Atypical appearance of hemangiomas is well known including flash-enhancing hemangiomas; hemangiomas with peripheral dot-like enhancement; and sclerosed hemangiomas which may not show complete fill-in especially in the center even in delayed phase. These atypical variants of hemangiomas occurring in fatty livers may pose difficulty in differentiation from metastases and primary lesions.

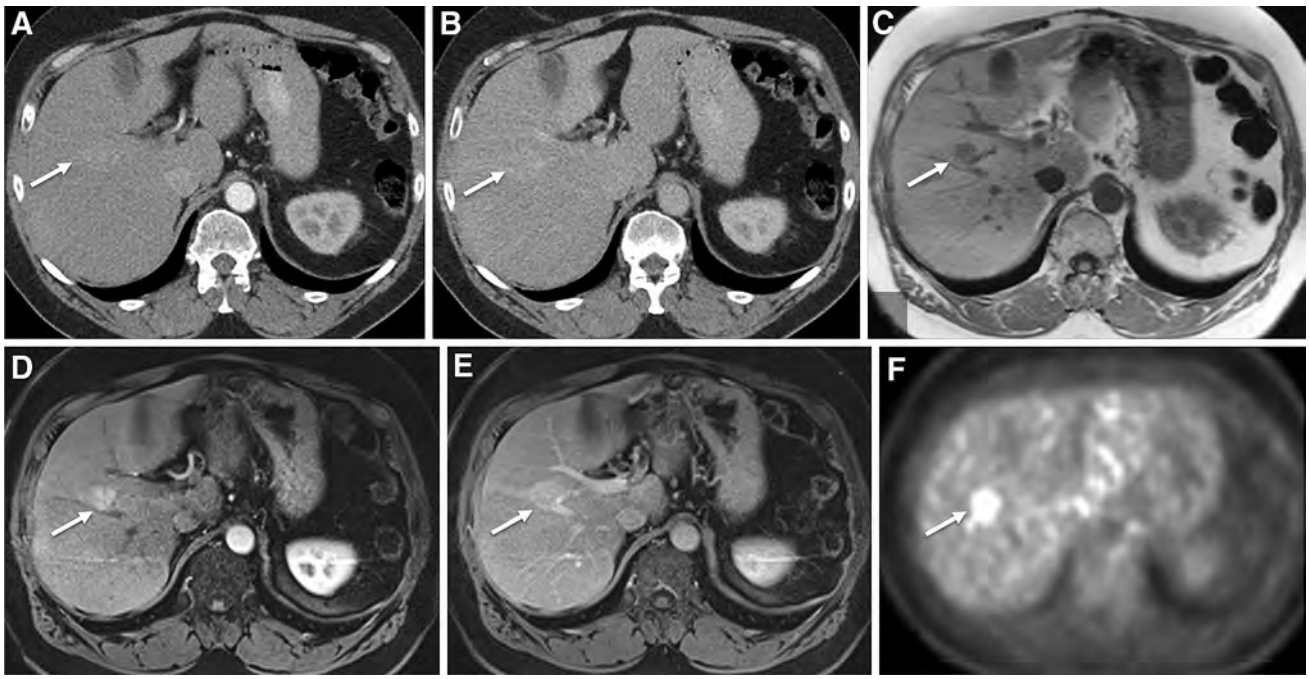

Fig. 11. Neuroendocrine metastases in fatty liver in a 64-year-old man. Arterial phase (**A**) and portal venous phase (**B**) CT showing a subtle enhancing lesion in the right lobe of liver (*arrow*) but difficult to detect on portal venous phase. T1-weighted MRI image (**C**) clearly shows hypointense lesion that demonstrates enhancement in both arterial (**D**) and portal venous (**E**) phases. FDG-PET (**F**) showing increased uptake in the lesion (*arrow*).

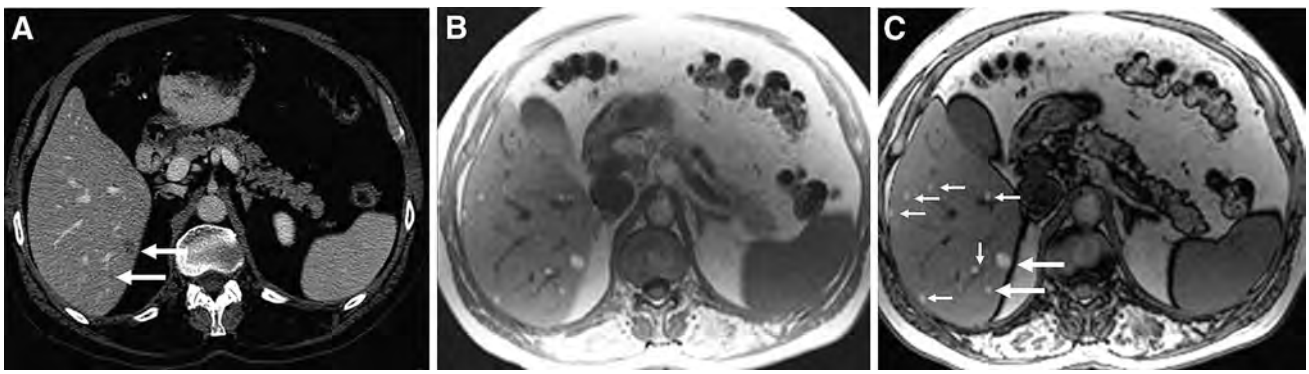

Fig. 12. Detection of focal lesions in liver on CT and MRI. A 64-year-old man with ocular melanoma with multiple metastases in a diffusely fatty liver. Corresponding CT and In- (**B**) and opposed phase (**C**) MRI sections performed 2 weeks apart. Only two lesions (*arrows*) are identified on this section in portal venous phase CT (**A**). Multiple smaller hyperintense lesions (*small arrows*, **C**) in the liver not identifiable on CT are demonstrated on the MRI images.

Focal nodular hyperplasia (FNH)

FNHs are composed of normal functioning hepatocytes and often have characteristic central scar. On US, FNHs are usually isoechoic or slightly hypoechoic to the normal liver and are often missed (stealth lesions) unless they are large and cause displacement of normal landmarks or vessels. The echogenic fatty liver may provide a good contrast for the detection of the relatively hypoechoic FNH and become conspicuous in a fatty liver. Definite diagnosis of FNH is usually made on contrast-enhanced CT and MRI. FNHs are classically isodense on CT in all phases except the arterial phase (Fig. 14) when they show intense hyperenhancement. However, in a fatty liver, FNH can be hyperdense in all phases and hence may not fit the classical description (Fig. 14). On MRI, FNH occurring in normal liver is most conspicuous in the arterial phase and may be difficult to identify in other phases and pulse sequences. However, in a fatty liver, FNH on MRI is well demonstrated with the use of fat-suppressed sequences, and they may appear hyper-

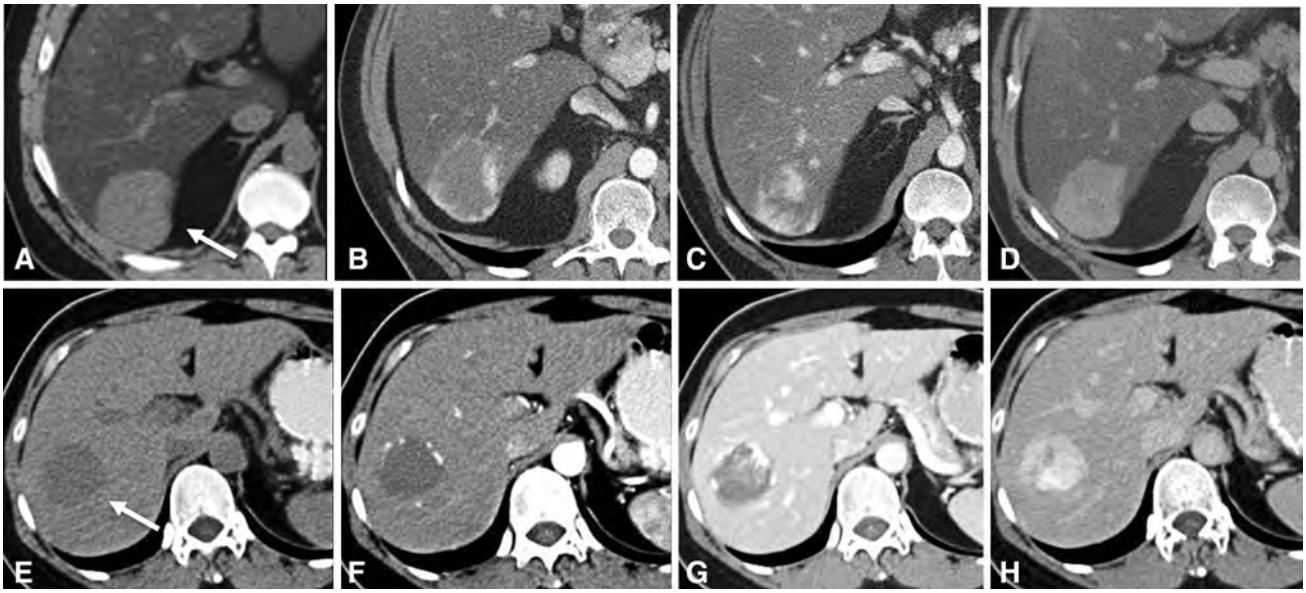

Fig. 13. Hemangioma in fatty liver (*top row*) and non-fatty liver (*bottom row*). Non-contrast (**A**, **E**), arterial phase (**B**, **F**), portal venous phase (**C**, **G**), and delayed phase (**D**, **H**) CT scans. The hemangioma in fatty liver is hyperdense (**A** *arrow*), whereas the hemangioma in non-fatty liver is hypodense (**E** *arrow*). Both hemangiomas show typical peripheral nodular enhancement in arterial phase, gradual fill-in during portal venous and nearly completely fill-in in the delayed phases.

intense in all contrast-enhanced phases (Fig. 14). Contrast-enhanced images should be reviewed with unenhanced images to understand the enhanced appearance for a correct diagnosis of FNH in fatty liver. Demonstration of central scar would increase confidence. Another helpful feature may be the demonstration of hyperintense perilesional ring during equilibrium phase and low-signal intensity rim-like appearance in the hepatocyte phase referred to as pseudocapsule, and this is attributed to compressed hepatic parenchyma [50, 51].Uncommonly, FNH may also have fat content when occurring in a fatty liver [52]. The appearance on imaging would then depend on the differences in fat content with hepatic parenchyma. Gadoxetate sodium (Gd-EOB-DTPA, Eovist) or Gd-BOPTA (MultiHance)-enhanced hepatobiliary phase shows characteristic uptake of contrast by focal nodular hyperplasia and is diagnostic. This would be useful for the confirmation of FNH. However, inflammatory adenomas can show the uptake of Gadoxetate and mimic FNH. Histological confirmation may occasionally be required to establish diagnosis and differentiate from adenoma.

Hepatocellular adenoma (HCA)

HCAs often contain fat, hemorrhage, necrosis, or calcification. The histological variants of HCAs have recently undergone revision, and currently four different types of HCAs are recognized. The four subtypes are as follows: (1) inflammatory HCAs are the most common type accounting for nearly half of HCAs and tend to be hypervascular with a tendency to bleed. They are associated with obesity, hepatic steatosis, and alcohol. On imaging, they show characteristic atoll sign and variable uptake of Gd-EOB-DTPA. This type is also associated with malignant transformation into HCCs; (2) HCAs with HNF-1-α mutation are typically fatty HCAs and associated with adenomatosis; (3) HCAs with β-catenin mutation are associated with high risk of transformation into HCC and are frequently seen in glycogen storage disorders and male hormone excess; and (4) an unclassified type which does not fit any of the above three groups [53]. HCA appearance therefore is variable and steatotic HCAs may blend in with fatty livers especially if they do not cause any mass effect. HCA with fat or recent hemorrhage may be hyperechoic or isoechoic to non-fatty liver on US. The echogenic fatty liver can again provide a better lesion-to-liver contrast for detection of a relatively hypoechoic HCA. Conversely, a fat-containing HCA may be difficult to detect in a fatty liver. On MRI, however, detection of smaller lesions may be improved with fat-suppressed sequences and the lesion may appear hyperenhanced in all dynamic phases (Fig. 15). Fat-containing HCA may pose problems, especially when similar to rest of the liver and sometimes may not be distinguishable from other fat-containing FLLs such as HCCs, angiomyolipoma, or lipoma. Correlation with the use of anabolic steroids or oral contraceptives, along with follow-up imaging to show stability and rarely biopsy may be required to establish diagnosis.

Hepatocellular carcinoma (HCC)

HCC is the most common primary malignant tumor of the liver. Emerging evidence suggests that there is in-

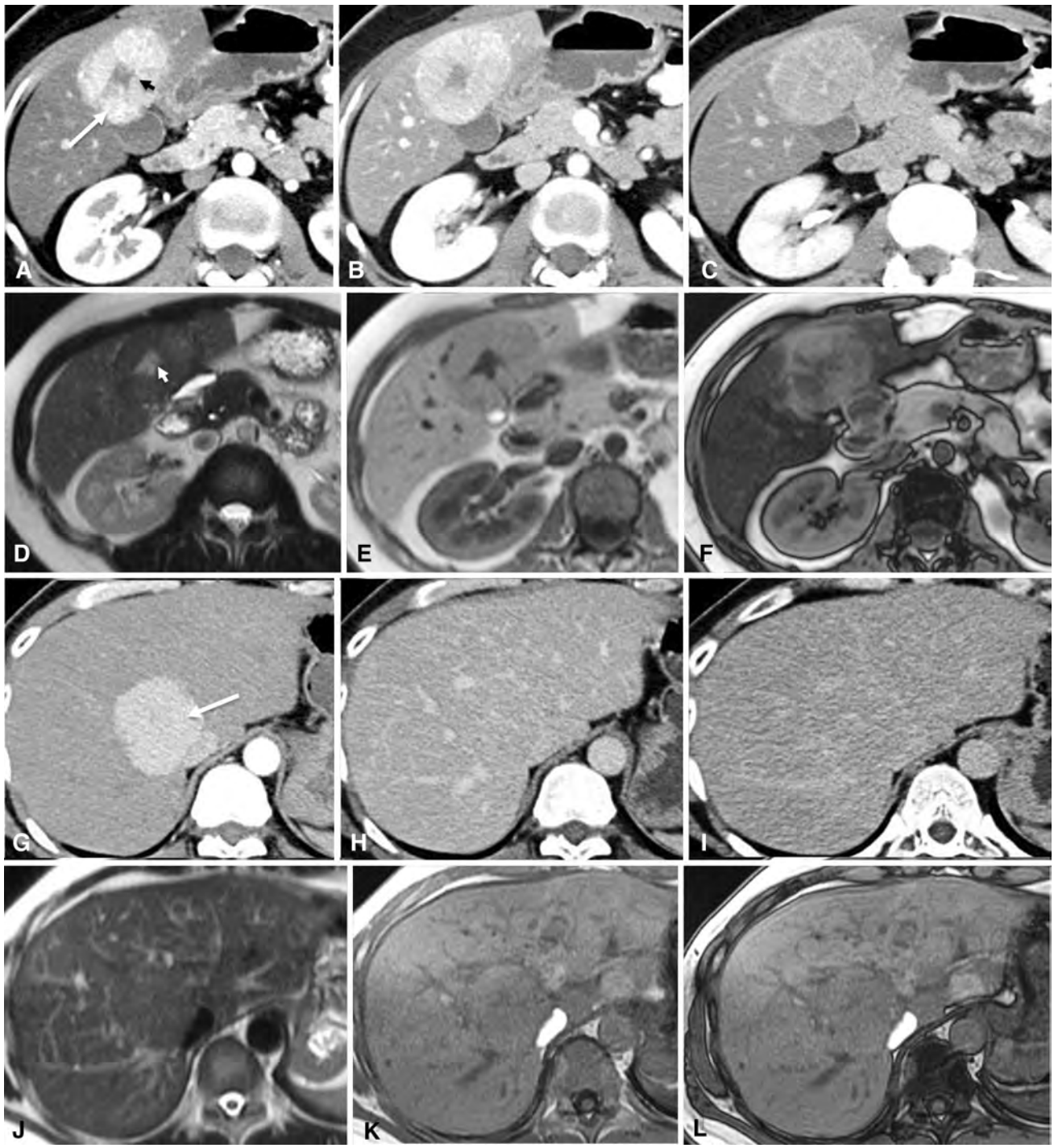

Fig. 14. Focal nodular hyperplasia. CT images (*top row*) and MRI images (*second row*) in a 41-year-old woman with fatty liver and FNH. The FNH (**A** *arrow*) shows intense hyperenhancement in arterial phase (**A**) and remains hyperintense to background liver in portal venous (**B**) and delayed (**C**) phases. The central non-enhancing region (*arrow head* **A**) corresponds to scar on T2-weighted MR image (*arrow head* **D**). In-phase (**E**) and opposed (**F**)-phase images show diffuse fatty change in the liver and some fatty change in the FNH also. Compare this with FNH occurring in normal liver in a 43-year-old man. Contrast-enhanced arterial phase CT image (**G**) shows hyperenhancing FNH (*arrow*) that becomes isodense to liver on portal venous (**H**) and delayed (**I**) phases. Note the lesion is isointense to liver parenchyma on T2-weighted image (**J**), in-phase (**K**), and opposed-phase (**L**) images. No fatty change in liver parenchyma.

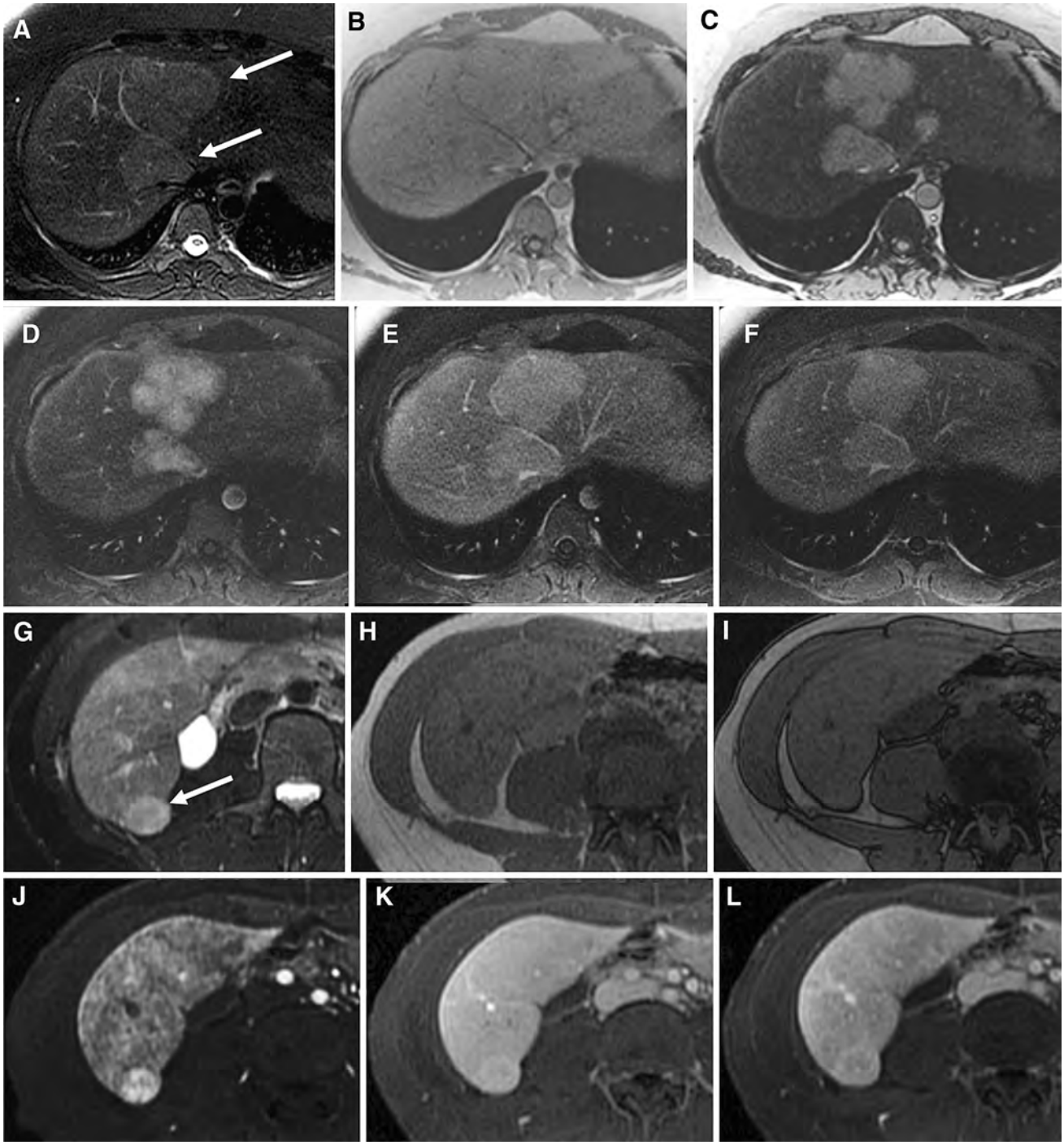

Fig. 15. Hepatocellular adenomas. A 35-year-old woman with multiple inflammatory adenomas. Axial fat-suppressed T2-weighted image (**A**) showing two mildly hyperintense lesions in the right lobe. In (**B**) and opposed-phase (**C**) images showing diffuse fatty change in the liver and a small third lesion. The lesions show arterial phase (**D**) hyperenhancement and remain hyperintense in portal venous (**E**) and delayed phase (**F**) images. In contrast to this is a beta catenin-negative adenoma in a 49-year-old woman. The adenoma is hyperintense on fat-suppressed T2-weighted image (*arrow* **G**) with no signal loss in in- (**H**) and opposed (**I**)-phase images demonstrating hyperenhancement in arterial phase (**J**) and becomes isointense in portal venous phase (**K**) with some washout in delayed phase (**L**).

creased incidence of HCC in NAFLD and even in the absence of cirrhosis [54]. An association between HCA transformation into HCC and metabolic syndrome is described [55]. Inflammatory type HCA is particularly associated with increased transformation into HCC and occurs more frequently in obesity [56]. HCCs occurring

in NAFLD tend to be larger, moderately or well-differentiated, and pseudocapsule is less often present [57]. HCC generally appears hypoechoic to non-fatty liver similar to other common FLLs. Detection and characterization of small HCC in a nodular liver can be challenging; however, diffuse fatty change often provides a better contrast on US and it may be easier to detect smaller HCCs. On CT and MRI, HCCs are characterized by arterial phase hyperenhancement and washout in portal venous or delayed phases according to published guidelines and criteria [58, 59]. However, in a fatty liver, although arterial phase enhancement is seen well against a hypodense fatty liver, washout may be difficult to appreciate (Fig. 16) as HCC may remain hyperdense or isodense in portal venous and delayed phases. Therefore, standard guidelines [58–61] for diagnosis of HCC may not be applicable in a fatty liver. Similar difficulty can occur on MRI using fat suppression post-contrast-enhanced sequences (Fig. 17). However, fat-suppressed T1-weighted sequences are part of standard liver MRI protocols in nearly all institutions. Recognition of fatty change in liver in pre-contrast sequences is therefore important. Subtracted dynamic phase images may be useful in some cases. Features of chronic liver disease, ancillary findings of portal hypertension, and elevated serum alpha fetoprotein levels are useful for diagnosis of HCC in such situations. In view of the global prevalence of NAFLD and increased incidence of HCCs in non-cirrhotic fatty liver, a separate diagnostic criteria for HCC in fatty liver may very soon be required.

Cholangiocarcinoma (CCA)

CCAs often have fibrosis component in the center of the tumor. On CT, CCAs typically are hypodense and show early peripheral enhancement with delayed central enhancement. They may be difficult to detect in hypodense fatty liver on non-contrast-enhanced CT (Fig. 18). Also, contrast filling in of the lesion in delayed phases in small CCA may be indistinguishable from a hemangioma. On MRI, CCA may be T2 hyperintense or hypointense lesions. The lesion may be well demonstrated on fat-suppressed post-contrast-enhanced MRI sequences in a fatty liver (Fig. 18). The typical enhancement pattern may be well seen on post-contrast images; however, the features may overlap with hemangiomas. Presence of other features such as biliary strictures and retraction of liver capsule may be useful for diagnosis of CCA in fatty livers.

Metastases

Perhaps the greatest impact of fatty change in liver is in the detection of metastases. Hepatic metastases have variable appearances depending on the primary. On US, lesions are generally better seen against a hyperechoic fatty liver (Fig. 19). However, if fatty change is severe, visualization of the deeper regions of the liver may be hampered (Fig. 9) and small metastases may not be detectable [62, 63]. On CT, hypervascular metastases can be better detected against a hypodense fatty liver, whereas hypodense/hypovascular metastases such as those from breast and colorectal carcinoma can appear isodense or hypodense in a fatty liver particularly on portal venous phase when both fatty liver and metastases may have similar densities [47, 48]. MRI with the use of fat-suppressed sequences (Fig. 19) is particularly helpful in the detection and assessment of metastases (Fig. 8). However on fat-suppressed images, hypointense metastases may not be detectable against fatty liver. In-phase imaging and/or non-fat-suppressed images may be needed to detect these lesions. FFCs and FFS may mimic multiple metastases on US and CT (Figs. 4, 7), and the nature of these lesions can be easily confirmed with MRI using fat-suppressed sequences, and the location of lesions is characteristic. Livers often undergo fatty change following chemotherapy either as a side effect of drugs or due to chemotherapy-associated steatohepatitis (CASH). Metastases initially hypodense/hypointense may be difficult to identify on a follow-up scan due to fatty change. Use of fat-suppressed sequences on MRI or multiphase imaging on CT may be useful. In the setting of fatty change, MRI is a better modality for evaluation of metastases, particularly useful for smaller metastatic lesions. Studies have shown superior performance of MRI in small (<1 cm) colorectal metastases [48] and with the use of Gd-EOB-DTPA [47].

Fat-containing FLLs

Fat within a lesion can be characteristic. Rare tumors like lipoma (Fig. 20) and angiomyolipoma (Fig. 21) contain large proportion of fat. These lesions tend to be incidentally detected and may be difficult to distinguish from more common HCA and HCCs and diagnosis is usually established by biopsy. Presence of fat within metastases is extremely rare. Metastatic ovarian teratomas, teratomas, liposarcoma, Wilms tumor, and renal cell carcinoma can give rise to fat-containing metastases [64, 65]. Knowledge of primary tumor is useful in arriving at diagnosis and may require biopsy.

Positron emission tomography (PET) in fatty liver

Several studies have reported variable uptake of ^{18}F-FDG-PET tracer in fatty livers [66–70]. Keramida et al. [69] proposed that FDG uptake increase in hepatic steatosis probably results from irreversible uptake in inflammatory cells secondary to steatohepatitis. Another study has shown that increased hepatic FDG uptake is associated with risk of cardiovascular events in patients with NAFLD [71]. These studies suggest a possible role of PET in differentiating steatohepatitis from simple

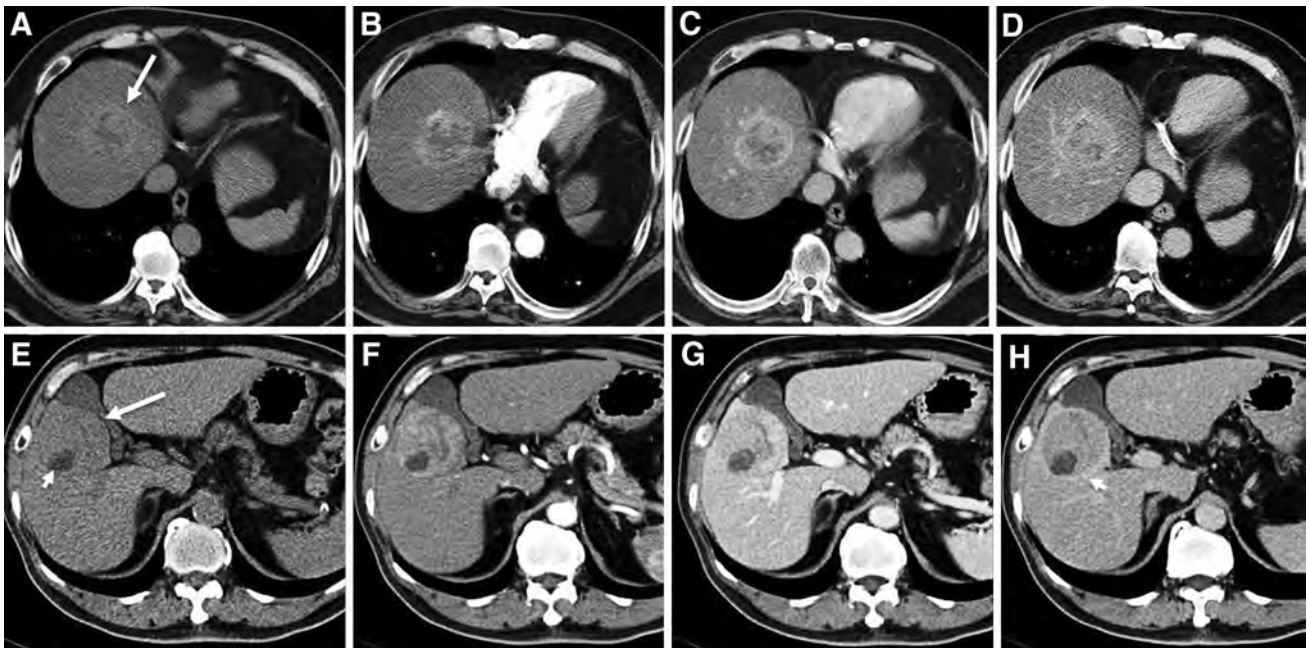

Fig. 16. CT appearances of histologically confirmed hepatocellular carcinomas (HCCs) in fatty liver (*top rows*) and non-fatty liver (*bottom row*). Non-contrast (**A**, **E**), arterial (**B**, **F**), portal venous (**C**, **G**), and delayed (**D**, **H**) phase CT scans. HCCs appear iso-hyperdense in fatty liver (*arrows* in **A**) and iso- to hypodense in non-fatty liver (*arrow* **E**). Note small fat component within the HCC (*arrowhead* **E**). Both HCCs show arterial phase hyperenhancement. HCC in fatty liver remains hyperdense to liver in portal venous and delayed phases, whereas HCC in non-fatty liver shows typical portal venous and delayed phase washout and pseudocapsule (*arrowhead* **H**).

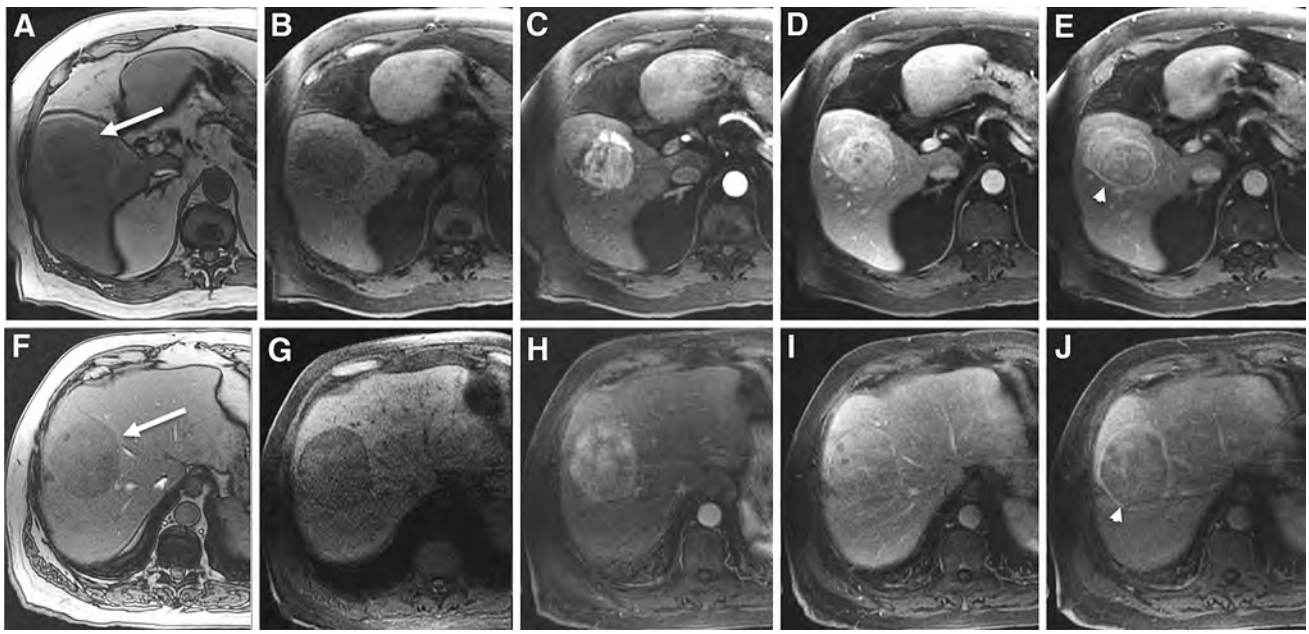

Fig. 17. MRI of HCC in fatty (*top row*) and non-fatty liver (*bottom row*). Axial opposed-phase T1 (**A**, **F**), pre-contrast T1 (**B**, **G**), late arterial phase (**C**, **H**), portal venous phase (**D**, **I**), and delayed phase (**E**, **J**) images. Note HCC in fatty liver appears isointense on opposed-phase image (**A** *arrow*) and hypointense in pre-contrast image (**B**) and hyperintense in all three post-contrast phases in contrast to typical HCC in non-fatty liver that is hypointense in pre-contrast images, hyperintense in arterial phase, washes out in portal venous and delayed phases, and with a pseudocapsule in delayed phase (*arrowhead* **J**). Pseudocapsule is also seen in HCC in fatty liver (*arrow head* **E**).

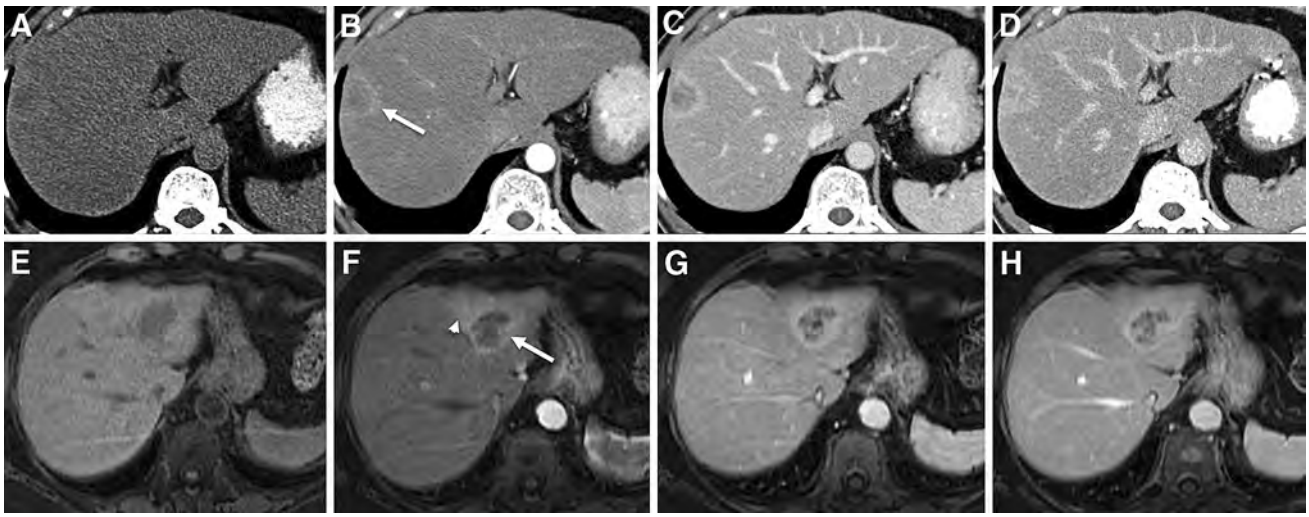

Fig. 18. Cholangiocarcinoma in fatty livers on CT (*top row*) and MRI (*bottom row*). Unenhanced (**A**, **E**), post-contrast arterial phase (**B**, **F**), portal venous phase (**C**, **G**), and delayed phase (**D**, **H**) showing peripheral rim-like enhancement in arterial phase and delayed central heterogeneous enhancement. Note segmental hyper perfusion (**F** *arrow head*) distal to tumor in arterial phase (**F** *arrow*).

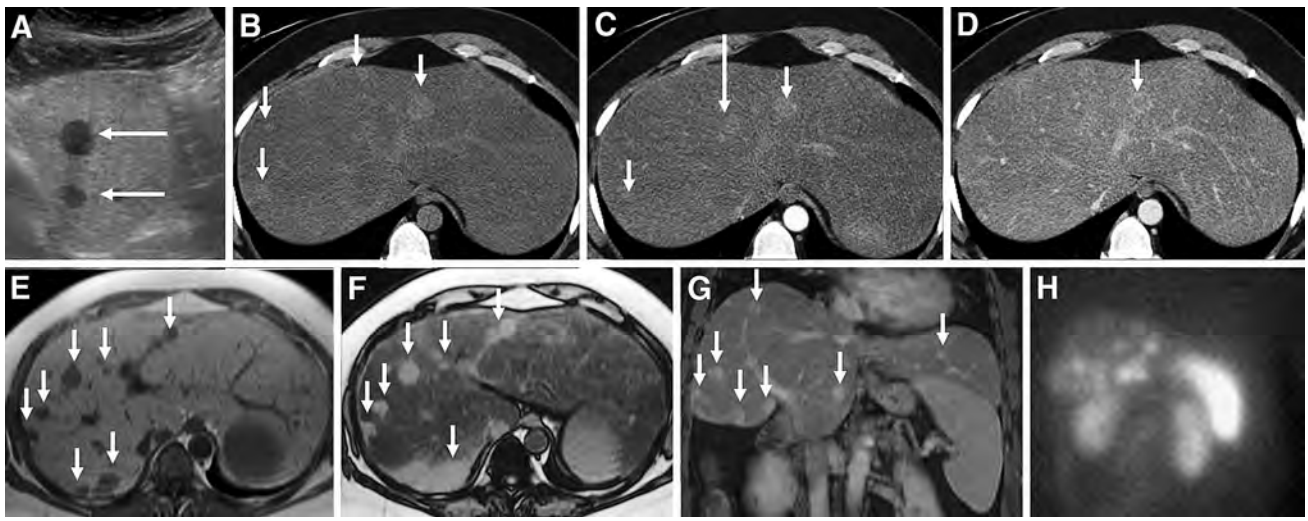

Fig. 19. Neuroendocrine metastases in a fatty liver. The metastases are hypoechoic to fatty liver parenchyma on ultrasound (*arrows* **A**). Non-contrast-enhanced CT (**B**) shows several nodules (*arrow heads*), and additional metastases are identified (*arrow*) in arterial phase (**C**). However, in the portal venous phase (**D**) only the larger lesion in the left lobe (*arrow head*) is discretely visualized. In-phase (**E**) and opposed-phase (**F**) MRI images showing several nodules, and post-contrast fat-suppressed T1-weighted coronal image (**G**) showing several enhancing nodules. PET scan (**H**) confirmed multiple metastatic lesions in the liver.

hepatic steatosis but it remains to be confirmed in a prospective and larger clinical study. Both FFC and FFS have been shown to be associated with high FDG uptake and mimickers of malignancy on PET/CT [72–76] posing diagnostic challenge especially in the work-up of patients with known primary malignancy elsewhere. Utility of MRI with demonstration of focal changes on fat suppression sequences and demonstration of uptake of Gd-EOB-DTPA may be useful to confirm that these lesions are either normal liver parenchyma or regions of fatty change. In general, PET/CT is useful in evaluation of metastatic lesions; however, reduced sensitivity of PET in the evaluation of colorectal liver metastases following neoadjuvant chemotherapy has been reported [46, 77] and this is likely due to chemotherapy-associated steatohepatitis and/or sinusoidal obstruction syndrome. More studies in patients who develop chemotherapy-associated steatosis and steatohepatitis are needed to con-

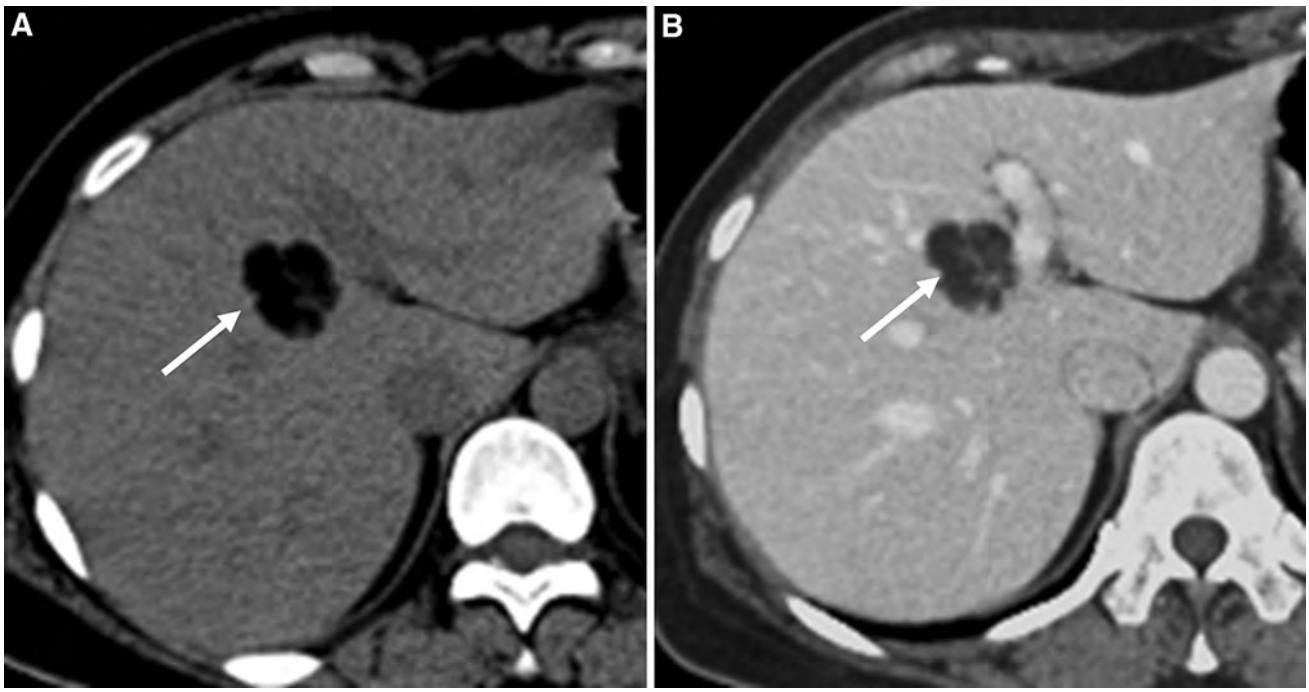

Fig. 20. Lipoma of liver. Axial non-contrast-enhanced (**A**) and contrast-enhanced CT (**B**) showing a lipoma (*arrow*). Biopsy was consistent with lipoma with elements of extramedullary hemopoiesis.

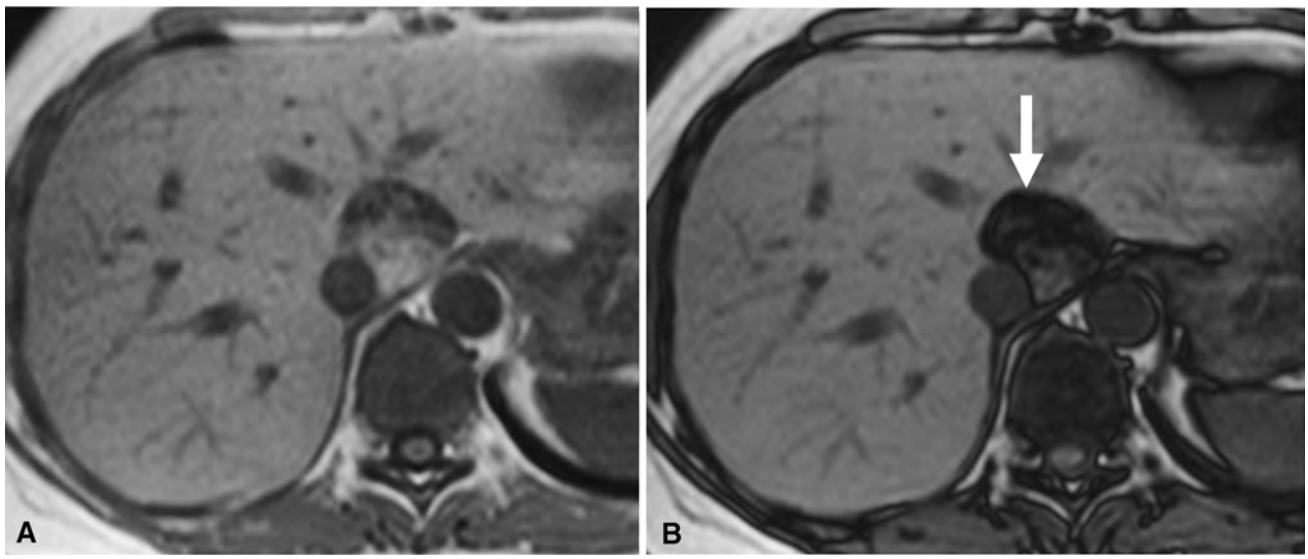

Fig. 21. Angiomyolipoma of liver. T1-weighted In-phase (**A**) and opposed-phase (**B**) MRI images demonstrating heterogeneous signal intensity mass in the caudate lobe of liver (*arrow*) with areas of loss of signal in opposed phase consistent with fat content in a histologically confirmed angiomyolipoma.

firm this limitation. A multi-modality approach like PET-MRI may be useful in patients with malignant disease and fatty livers.

Conclusion

Fatty change in the liver influences both detection and characterization of FLL. Knowledge of characteristic features and typical distribution sites of FFC and FFS are important to differentiate these processes from true hepatic lesions. In the setting of focal and diffuse fatty liver, sensitivity for FLL detection is generally superior using MRI rather than a single-portal venous phase CT. Because the sensitivity of single-phase (portal venous) CT is compromised for the detection of FLL in the set-

ting of fatty change, unenhanced CT and/or multiphasic imaging may be useful.

Imaging appearances of FLLs may be different when occurring in a fatty liver as opposed to normal liver, such that imaging findings no longer correspond to fit the typical description. Post-contrast relative enhancement features may be significantly altered by fatty change, and standard guidelines for characterization may not be applicable. The features should be interpreted taking into account the fatty change in the liver. Guidelines for imaging criteria for important lesions like HCC perhaps should be modified to incorporate lesions occurring in fatty liver.

Compliance with ethical standards

Funding No funding was received for this study.

Conflict of interest The authors declare that they have no conflict of interest.

Ethical approval All procedures performed in studies involving human participants were in accordance with the ethical standards of the institutional and/or national research committee and with the 1964 Helsinki declaration and its later amendments or comparable ethical standards. For this type of study formal consent is not required.

Informed consent Informed consent was waived for this retrospective review of images.

References

1. Vernon G, Baranova A, Younossi ZM (2011) Systematic review: the epidemiology and natural history of non-alcoholic fatty liver disease and non-alcoholic steatohepatitis in adults. Aliment Pharmacol Ther 34:274–285
2. Boyce CJ, Pickhardt PJ, Kim DH, et al. (2010) Hepatic steatosis (fatty liver disease) in asymptomatic adults identified by unenhanced low-dose CT. AJR Am J Roentgenol 194:623–628
3. Ong JP, Elariny H, Collantes R, et al. (2005) Predictors of nonalcoholic steatohepatitis and advanced fibrosis in morbidly obese patients. Obes Surg 15:310–315
4. Paredes AH, Torres DM, Harrison SA (2012) Nonalcoholic fatty liver disease. Clin Liver Dis 16:397–419
5. Lazo M, Clark JM (2008) The epidemiology of nonalcoholic fatty liver disease: a global perspective. Semin Liver Dis 28:339–350
6. Younossi ZM, Stepanova M, Afendy M, et al. (2011) Changes in the prevalence of the most common causes of chronic liver diseases in the United States from 1988 to 2008. Clin Gastroenterol Hepatol 9:524–530 ((e521; quiz e560))
7. Hamaguchi M, Kojima T, Takeda N, et al. (2005) The metabolic syndrome as a predictor of nonalcoholic fatty liver disease. Ann Intern Med 143:722–728
8. Hamer OW, Aguirre DA, Casola G, et al. (2006) Fatty liver: imaging patterns and pitfalls. Radiographics 26:1637–1653
9. Wilson SR, Rosen IE, Chin-Sang HB, Arenson AM (1982) Fatty infiltration of the liver—an imaging challenge. J Can Assoc Radiol 33:227–232
10. Bashist B, Hecht HL, Harley WD (1982) Computed tomographic demonstration of rapid changes in fatty infiltration of the liver. Radiology 142:691–692
11. Brunt EM (2007) Pathology of fatty liver disease. Mod Pathol 20(Suppl 1):S40–S48
12. Quinn SF, Gosink BB (1985) Characteristic sonographic signs of hepatic fatty infiltration. AJR Am J Roentgenol 145:753–755
13. Onishi H, Theisen D, Dietrich O, Reiser MF, Zech CJ (2014) Hepatic steatosis: effect on hepatocyte enhancement with gadoxetate disodium-enhanced liver MR imaging. J Magn Reson Imaging 39:42–50
14. Schwenzer NF, Springer F, Schraml C, et al. (2009) Non-invasive assessment and quantification of liver steatosis by ultrasound, computed tomography and magnetic resonance. J Hepatol 51:433–445
15. Fishbein M, Castro F, Cheruku S, et al. (2005) Hepatic MRI for fat quantitation: its relationship to fat morphology, diagnosis, and ultrasound. J Clin Gastroenterol 39:619–625
16. Needleman L, Kurtz AB, Rifkin MD, et al. (1986) Sonography of diffuse benign liver disease: accuracy of pattern recognition and grading. AJR Am J Roentgenol 146:1011–1015
17. Strauss S, Gavish E, Gottlieb P, Katsnelson L (2007) Interobserver and intraobserver variability in the sonographic assessment of fatty liver. AJR Am J Roentgenol 189:W320–W323
18. Sasso M, Beaugrand M, de Ledinghen V, et al. (2010) Controlled attenuation parameter (CAP): a novel VCTE^{TM} guided ultrasonic attenuation measurement for the evaluation of hepatic steatosis: preliminary study and validation in a cohort of patients with chronic liver disease from various causes. Ultrasound Med Biol 36:1825–1835
19. Limanond P, Raman SS, Lassman C, et al. (2004) Macrovesicular hepatic steatosis in living related liver donors: correlation between CT and histologic findings. Radiology 230:276–280
20. Piekarski J, Goldberg HI, Royal SA, Axel L, Moss AA (1980) Difference between liver and spleen CT numbers in the normal adult: its usefulness in predicting the presence of diffuse liver disease. Radiology 137:727–729
21. Ricci C, Longo R, Gioulis E, et al. (1997) Noninvasive in vivo quantitative assessment of fat content in human liver. J Hepatol 27:108–113
22. Johnston RJ, Stamm ER, Lewin JM, Hendrick RE, Archer PG (1998) Diagnosis of fatty infiltration of the liver on contrast enhanced CT: limitations of liver-minus-spleen attenuation difference measurements. Abdom Imaging 23:409–415
23. Reeder SB, Cruite I, Hamilton G, Sirlin CB (2011) Quantitative assessment of liver fat with magnetic resonance imaging and spectroscopy. J Magn Reson Imaging 34:729–749
24. Yu H, McKenzie CA, Shimakawa A, et al. (2007) Multiecho reconstruction for simultaneous water-fat decomposition and T2* estimation. J Magn Reson Imaging 26:1153–1161
25. Reeder SB, Hu HH, Sirlin CB (2012) Proton density fat-fraction: a standardized MR-based biomarker of tissue fat concentration. J Magn Reson Imaging 36:1011–1014
26. Cassidy FH, Yokoo T, Aganovic L, et al. (2009) Fatty liver disease: MR imaging techniques for the detection and quantification of liver steatosis. Radiographics 29:231–260
27. Yu H, Shimakawa A, McKenzie CA, et al. (2008) Multiecho water-fat separation and simultaneous R2* estimation with multifrequency fat spectrum modeling. Magn Reson Med 60:1122–1134
28. Yu H, Shimakawa A, Hines CD, et al. (2011) Combination of complex-based and magnitude-based multiecho water-fat separation for accurate quantification of fat-fraction. Magn Reson Med 66:199–206
29. Décarie PO, Lepanto L, Billiard JS, et al. (2011) Fatty liver deposition and sparing: a pictorial review. Insights Imaging 2:533–538
30. Hamer OW, Aguirre DA, Casola G, Sirlin CB (2005) Imaging features of perivascular fatty infiltration of the liver: initial observations. Radiology 237:159–169
31. Kröncke TJ, Taupitz M, Kivelitz D, et al. (2000) Multifocal nodular fatty infiltration of the liver mimicking metastatic disease on CT: imaging findings and diagnosis using MR imaging. Eur Radiol 10:1095–1100
32. Sohn J, Siegelman E, Osiason A (2001) Unusual patterns of hepatic steatosis caused by the local effect of insulin revealed on chemical shift MR imaging. AJR Am J Roentgenol 176:471–474
33. Valls C, Iannacconne R, Alba E, et al. (2006) Fat in the liver: diagnosis and characterization. Eur Radiol 16:2292–2308
34. Marin D, Iannaccone R, Catalano C, Passariello R (2006) Multinodular focal fatty infiltration of the liver: atypical imaging findings on delayed T1-weighted Gd-BOPTA-enhanced liver-specific MR images. J Magn Reson Imaging 24:690–694
35. Yeom SK, Byun JH, Kim HJ, et al. (2013) Focal fat deposition at liver MRI with gadobenate dimeglumine and gadoxetic acid:

quantitative and qualitative analysis. Magn Reson Imaging 31:911–917
36. Matsui O, Kadoya M, Takahashi S, et al. (1995) Focal sparing of segment IV in fatty livers shown by sonography and CT: correlation with aberrant gastric venous drainage. AJR Am J Roentgenol 164:1137–1140
37. Tom WW, Yeh BM, Cheng JC, et al. (2004) Hepatic pseudotumor due to nodular fatty sparing: the diagnostic role of opposed-phase MRI. AJR Am J Roentgenol 183:721–724
38. Itai Y (2000) Peritumoral sparing of fatty liver: another important instance of focal sparing caused by a hepatic tumor. AJR Am J Roentgenol 174:868–870
39. Grossholz M, Terrier F, Rubbia L, et al. (1998) Focal sparing in the fatty liver as a sign of an adjacent space-occupying lesion. AJR Am J Roentgenol 171:1391–1395
40. Chung JJ, Kim MJ, Kim JH, Lee JT, Yoo HS (2003) Fat sparing of surrounding liver from metastasis in patients with fatty liver: MR imaging with histopathologic correlation. AJR Am J Roentgenol 180:1347–1350
41. Gabata T, Kadoya M, Matsui O, et al. (2001) Peritumoral spared area in fatty liver: correlation between opposed-phase gradient-echo MR imaging and CT arteriography. Abdom Imaging 26:384–389
42. Martí-Bonmatí L, Peñaloza F, Villarreal E, Martinez MJ (2005) Nonspecificity of the fat-sparing ring surrounding focal liver lesion at MR imaging. Acad Radiol 12:1551–1556
43. Torres DM, Harrison SA (2012) Nonalcoholic steatohepatitis and noncirrhotic hepatocellular carcinoma: fertile soil. Semin Liver Dis 32:30–38
44. Baffy G, Brunt EM, Caldwell SH (2012) Hepatocellular carcinoma in non-alcoholic fatty liver disease: an emerging menace. J Hepatol 56:1384–1391
45. Schütte K, Schulz C, Poranzke J, et al. (2014) Characterization and prognosis of patients with hepatocellular carcinoma (HCC) in the non-cirrhotic liver. BMC Gastroenterol 14:117
46. van Kessel CS, Buckens CF, van den Bosch MA, et al. (2012) Preoperative imaging of colorectal liver metastases after neoadjuvant chemotherapy: a meta-analysis. Ann Surg Oncol 19:2805–2813
47. Berger-Kulemann V, Schima W, Baroud S, et al. (2012) Gadoxetic acid-enhanced 3.0 T MR imaging versus multidetector-row CT in the detection of colorectal metastases in fatty liver using intraoperative ultrasound and histopathology as a standard of reference. Eur J Surg Oncol 38:670–676
48. Kulemann V, Schima W, Tamandl D, et al. (2011) Preoperative detection of colorectal liver metastases in fatty liver: MDCT or MRI? Eur J Radiol 79:e1–e6
49. Reiter MJ, Hannemann NP, Schwope RB, Lisanti CJ, Learn PA (2015) Role of imaging for patients with colorectal hepatic metastases: what the radiologist needs to know. Abdom Imaging 40:3029–3042
50. Goodwin MD, Dobson JE, Sirlin CB, Lim BG, Stella DL (2011) Diagnostic challenges and pitfalls in MR imaging with hepatocyte-specific contrast agents. Radiographics 31:1547–1568
51. Grazioli L, Morana G, Kirchin MA, Schneider G (2005) Accurate differentiation of focal nodular hyperplasia from hepatic adenoma at gadobenate dimeglumine-enhanced MR imaging: prospective study. Radiology 236:166–177
52. Ronot M, Paradis V, Duran R, et al. (2013) MR findings of steatotic focal nodular hyperplasia and comparison with other fatty tumours. Eur Radiol 23:914–923
53. Bioulac-Sage P, Rebouissou S, Thomas C, et al. (2007) Hepatocellular adenoma subtype classification using molecular markers and immunohistochemistry. Hepatology 46:740–748
54. Alexander J, Torbenson M, Wu TT, Yeh MM (2013) Non-alcoholic fatty liver disease contributes to hepatocarcinogenesis in non-cirrhotic liver: a clinical and pathological study. J Gastroenterol Hepatol 28:848–854
55. Farges O, Ferreira N, Dokmak S, et al. (2011) Changing trends in malignant transformation of hepatocellular adenoma. Gut 60:85–89
56. Chang CY, Hernandez-Prera JC, Roayaie S, Schwartz M, Thung SN (2013) Changing epidemiology of hepatocellular adenoma in the United States: review of the literature. Int J Hepatol 2013:604860
57. Iannaccone R, Piacentini F, Murakami T, et al. (2007) Hepatocellular carcinoma in patients with nonalcoholic fatty liver disease: helical CT and MR imaging findings with clinical-pathologic comparison. Radiology 243:422–430
58. Bruix J, Sherman M, Diseases AAftSoL (2011) Management of hepatocellular carcinoma: an update. Hepatology 53:1020–1022
59. Bruix J, Sherman M, Practice Guidelines Committee AeAftSoLD (2005) Management of hepatocellular carcinoma. Hepatology 42:1208–1236
60. Liver EAFTSOT, Cancer EOFRATO (2012) EASL-EORTC clinical practice guidelines: management of hepatocellular carcinoma. J Hepatol 56:908–943
61. Omata M, Lesmana LA, Tateishi R, et al. (2010) Asian Pacific Association for the Study of the Liver consensus recommendations on hepatocellular carcinoma. Hepatol Int 4:439–474
62. Wu S, Tu R, Nan R, et al. (2016) Impact of variations in fatty liver on sonographic detection of focal hepatic lesions originally identified by CT. Ultrasonography 35:39–46
63. Van Vledder MG, Boctor EM, Assumpcao LR, et al. (2010) Intraoperative ultrasound elasticity imaging for monitoring of hepatic tumour thermal ablation. HPB 12:717–723
64. Esensten ML, Shaw SL, Pak HY, Gildenhorn HL (1983) CT demonstration of multiple intraperitoneal teratomatous implants. J Comput Assist Tomogr 7:1117–1118
65. Basaran C, Karcaaltincaba M, Akata D, et al. (2005) Fat-containing lesions of the liver: cross-sectional imaging findings with emphasis on MRI. AJR Am J Roentgenol 184:1103–1110
66. Lin CY, Lin WY, Lin CC, et al. (2011) The negative impact of fatty liver on maximum standard uptake value of liver on FDG PET. Clin Imaging 35:437–441
67. Bural GG, Torigian DA, Burke A, et al. (2010) Quantitative assessment of the hepatic metabolic volume product in patients with diffuse hepatic steatosis and normal controls through use of FDG-PET and MR imaging: a novel concept. Mol Imaging Biol 12:233–239
68. Abele JT, Fung CI (2010) Effect of hepatic steatosis on liver FDG uptake measured in mean standard uptake values. Radiology 254:917–924
69. Keramida G, Potts J, Bush J, et al. (2014) Accumulation of (18)F-FDG in the liver in hepatic steatosis. AJR Am J Roentgenol 203:643–648
70. Abikhzer G, Alabed YZ, Azoulay L, Assayag J, Rush C (2011) Altered hepatic metabolic activity in patients with hepatic steatosis on FDG PET/CT. AJR Am J Roentgenol 196:176–180
71. Moon SH, Hong SP, Cho YS, et al. (2015) Hepatic FDG uptake is associated with future cardiovascular events in asymptomatic individuals with non-alcoholic fatty liver disease. J Nucl Cardiol. doi:10.1007/s12350-015-0297-y
72. Kim YH, Kim JY, Jang SJ, et al. (2011) F-18 FDG uptake in focal fatty infiltration of liver mimicking hepatic malignancy on PET/CT images. Clin Nucl Med 36:1146–1148
73. Le Y, Chen Y, Huang Z, Cai L, Zhang L (2014) Intense FDG activity in focal hepatic steatosis. Clin Nucl Med 39:669–672
74. Harisankar CN (2014) Focal fat sparing of the liver: a nonmalignant cause of focal FDG uptake on FDG PET/CT. Clin Nucl Med 39:e359–e361
75. Purandare NC, Rangarajan V, Rajnish A, et al. (2008) Focal fat spared area in the liver masquerading as hepatic metastasis on F-18 FDG PET imaging. Clin Nucl Med 33:802–805
76. Han N, Feng H, Arnous MM, Bouhari A, Lan X (2016) Multiple liver focal fat sparing lesions with unexpectedly increased (18)F-FDG uptake mimicking metastases examined by ultrasound (18)F-FDG PET/CT and MRI. Hell J Nucl Med 19:173–175
77. Lubezky N, Metser U, Geva R, et al. (2007) The role and limitations of 18-fluoro-2-deoxy-D-glucose positron emission tomography (FDG-PET) scan and computerized tomography (CT) in restaging patients with hepatic colorectal metastases following neoadjuvant chemotherapy: comparison with operative and pathological findings. J Gastrointest Surg 11:472–478